

## The Firing of an Excitable Neuron in the Presence of Stochastic Trains of Strong Synaptic Inputs

**Jonathan Rubin**

*rubin@math.pitt.edu*

*Department of Mathematics, University of Pittsburgh, Pittsburgh, PA 15260 U.S.A.*

**Krešimir Josić**

*josic@math.uh.edu*

*Department of Mathematics, University of Houston, Houston,  
TX 77204-3008, U.S.A.*

We consider a fast-slow excitable system subject to a stochastic excitatory input train and show that under general conditions, its long-term behavior is captured by an irreducible Markov chain with a limiting distribution. This limiting distribution allows for the analytical calculation of the system's probability of firing in response to each input, the expected number of response failures between firings, and the distribution of slow variable values between firings. Moreover, using this approach, it is possible to understand why the system will not have a stationary distribution and why Monte Carlo simulations do not converge under certain conditions. The analytical calculations involved can be performed whenever the distribution of interexcitation intervals and the recovery dynamics of the slow variable are known. The method can be extended to other models that feature a single variable that builds up to a threshold where an instantaneous spike and reset occur. We also discuss how the Markov chain analysis generalizes to any pair of input trains, excitatory or inhibitory and synaptic or not, such that the frequencies of the two trains are sufficiently different from each other. We illustrate this analysis on a model thalamocortical (TC) cell subject to two example distributions of excitatory synaptic inputs in the cases of constant and rhythmic inhibition. The analysis shows a drastic drop in the likelihood of firing just after inhibitory onset in the case of rhythmic inhibition, relative even to the case of elevated but constant inhibition. This observation provides support for a possible mechanism for the induction of motor symptoms in Parkinson's disease and for their relief by deep brain stimulation, analyzed in Rubin and Terman (2004).

## 1 Introduction

---

There has been substantial discussion of the roles of excitatory and inhibitory synaptic inputs in driving or modulating neuronal firing. Computational analysis of this issue generally considers a neuron awash in a sea of synaptic bombardment (Somers et al., 1998; van Vreeswijk & Sompolinsky, 1998; De Schutter, 1999; Tiesinga, Jose, & Sejnowski, 2000; Tiesinga, 2005; Chance, Abbott, & Reyes, 2002; Tiesinga & Sejnowski, 2004; Huertas, Groff, & Smith, 2005). In this work, we also investigate the impact of synaptic inputs on the firing of a neuron, but with a focus on the effects of single inputs within stochastic trains. This investigation is motivated by consideration of thalamocortical relay (TC) cells, under the hypothesis that such cells are configured to reliably relay individual excitatory inputs, arising from either strong, isolated synaptic signals or tightly synchronized sets of synaptic signals, during states of attentive wakefulness, yet are also modulated by inhibitory input streams (Smith & Sherman, 2002). This viewpoint leads to the question of how different patterns of inhibitory modulation affect the relationship between the activity of a neuron and a stochastic excitatory input train that it receives.

The main goal of this letter is to introduce and illustrate a mathematical approach to the analysis of this relationship. Our approach applies to general excitable systems with separation of timescales, including a single slow variable and fast onset and offset of inputs. These ideas directly generalize to other neuronal models featuring a slow buildup of potential interrupted by instantaneous spikes and resets. We harness these features to reduce system dynamics to a one-dimensional map on the slow variable. Each iteration of the map corresponds to the time interval from the arrival of one excitatory input to the arrival of the next excitatory input (Othmer & Watanabe, 1994; Xie, Othmer, & Watanabe, 1996; Ichinose, Aihara, & Judd, 1998; Othmer & Xie, 1999; Coombes & Osbaldestin, 2000). From this map, under the assumption of a bounded excitatory input rate, we derive a transition process based on the evolution of the slow variable between inputs. In general, such a process would be non-Markovian, because the transition probabilities would depend on the arrival times of all inputs the cell had received since it last spiked. However, we derive an irreducible Markov chain by defining states that are indexed by both slow variable values and numbers of inputs received since last firing.

In the case of a constant inhibition level, we prove the key result that under rather general conditions, this Markov chain is aperiodic and hence has a limiting distribution. This limiting distribution can be computed from the distribution of input arrival times. Once obtained, it can be used to deduce much about the firing statistics of the driven cell, including the probability that the cell will fire in response to a given excitatory input, the expected number of response failures that the cell will experience between firings, and the distribution of slow variable values

attained after any fixed number of unsuccessful inputs arriving between firings.

We emphasize that, a priori, it is not certain that such a limiting distribution exists. Therefore, Monte Carlo methods, which rely on the assumed existence of a limit, may fail to converge and hence may give misleading results about firing statistics and the distribution of slow variable values at input arrival times. In addition to providing conditions that guarantee the existence of a limiting distribution for the Markov chain, our analysis shows how convergence failure can arise in the case of a stochastic train of excitatory inputs that is close to periodic. When our existence conditions are satisfied, our approach yields an analytical calculation of the limiting distribution, eliminating the need for simulations as well as the complications of transients and slow convergence, and the eigenvalues of the transition matrix used to compute the limiting distribution give information about convergence rate. Moreover, this approach provides a framework for the analysis of how changes in the statistics of the inputs affect the output of a cell. Finally, the Markov chain analysis allows for the identification of bifurcation events in which variation of model parameters can lead to abrupt changes that affect long-term statistics, although we do not pursue this in detail in this work (see Doi, Inoue, & Kumagai, 1998; Tateno & Jimbo, 2000, which we comment on in section 9).

We discuss the Markov chain approach in the particular case of constant inhibition, which may be zero or nonzero, and extend it to the case of inhibition that undergoes abrupt switches between two different levels, at a lower frequency than that of the excitatory signal. These choices are motivated by the analysis of TC cell relay reliability in the face of variations in inhibitory basal ganglia outputs that arise in Parkinson's disease (PD) and under deep brain stimulation (DBS), applied to combat the motor symptoms of PD. An important point emerging from experimental results is that parkinsonian changes induce rhythmicity in inhibitory basal ganglia outputs (Nini, Feingold, Slovin, & Bergman, 1995; Magnin, Morel, & Jeanmonod, 2000; Raz, Vaadia, & Bergman, 2000; Brown et al., 2001), while DBS regularizes these outputs, albeit at higher-than-normal levels (Anderson, Postpuna, & Ruffo, 2003; Hashimoto, Elder, Okun, Patrick, & Vitek, 2003). In recent work, Rubin and Terman (2004) provided computational and analytical support for the hypothesis that, given a TC cell that can respond reliably to excitatory inputs under normal conditions, the parkinsonian introduction of repetitive, fairly abrupt switches between high and low levels of inhibition to the TC cell will disrupt reliable relay. On the other hand, regularized basal ganglia activity, even if it leads to unusually high levels of inhibition, can restore reliable TC responses. While their computational results focused on finite time simulations of two TC models with particular choices of excitatory and inhibitory input strengths, frequencies, and durations, the general framework presented here can be used to analyze how a model TC cell responds to any train of fast excitatory inputs in

the presence of inhibition that stochastically makes abrupt jumps between two levels. Furthermore, the results of this letter yield more detailed statistical information about the firing of the driven TC cells, particularly just after the onset of inhibition.

The letter is organized as follows. In section 2, we review the way in which the dynamics of a fast-slow excitable system under pulsatile drive can be reduced to a map. In section 3, we use these ideas to construct a Markov chain that captures the relevant aspects of the dynamics of the system. We consider the existence of limiting densities for the constructed Markov chain and their interpretation in section 4. Further, we discuss the application of these ideas to responses of a population of cells, as well as their extension to populations with heterogeneities and to related models, in section 5. The specific example of determining the reliability of a reduced model TC cell under various types of inputs is addressed, as an application of the theory, in sections 6 and 7, while an explicit connection to PD and DBS is made in section 8. Some details of the calculations underlying the results of these sections are contained in the appendixes. Section 9 provides a summary of our results, a discussion of their relation to past work, and some ideas on possible generalization and future directions.

In the two examples that we present, one with a uniform and one with a normal distribution of excitatory inputs, a significant decrease in the responsiveness of the model TC cell and a significant increase in its likelihood of being found far from firing threshold result after the onset of the inhibitory phase of a time-varying inhibitory input, relative to the cases of high or low but constant inhibition. These findings are in agreement with Rubin and Terman (2004) and, based on the generality of our approach, appear to represent general characteristics of the TC model with a single slow variable.

## 2 Reduction of the Dynamics to Maps of the Interval ---

In this section we introduce a general relaxation oscillator subject to synaptic input. Under certain assumptions on the form of the input, the dynamics of the oscillator is accurately captured by a map of an interval.

**2.1 A General Relaxation Oscillator.** Consider a model system of the form

$$\begin{aligned} v' &= f(v, w) + I(v, t) \\ w' &= \varepsilon g(v, w), \end{aligned} \tag{2.1}$$

where  $0 < \varepsilon \ll 1$ . In the neuronal context, the fast variable  $v$  models the voltage, while the slow variable  $w$  typically models different conductances (Rubin & Terman, 2002). The input to the oscillator is modeled by the term

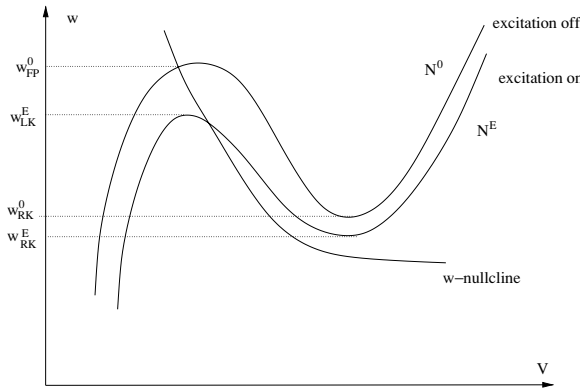


Figure 1: The nullclines of system 2.1 under the assumptions discussed in the text. The upper and lower  $v$ -nullclines correspond to  $s_{exc} = 0$  (excitation off) and  $s_{exc} = 1$  (excitation on), respectively.

$I(v, t)$ . We will assume that if  $I(v, t) = C$  for a constant  $C$  in a range of interest, then the  $v$ -nullcline, given implicitly by  $f(v, w) = -C$ , has a three-branched, or  $N$ -like, shape (see Figure 1). We will refer to the different branches of this nullcline as the left, middle, and right branch, respectively. Under assumptions on the form of  $f$  and  $g$  that typically hold in practice (Rubin & Terman, 2002), it is well known that if the  $w$ -nullcline, given implicitly by  $g(v, w) = 0$ , intersects the  $v$ -nullcline at the middle branch, then equation 2.1 has oscillatory solutions, known as relaxation oscillations. If the  $w$ -nullcline meets the  $v$ -nullcline at the left branch, then there are no oscillatory solutions, but the system is excitable. In this case, a kick in the positive  $v$  direction can trigger an extended excursion (a spike). In the following, we consider the case when the two nullclines intersect on the left branch of the  $v$ -nullcline in the absence of input.

In the work system presented here, equation 2.1 will be used as a model of a neuronal cell, and  $I(v, t)$  will model synaptic input, so that

$$I(v, t) = -g_{exc}s_{exc}(t)(v - v_{exc}) - g_{inh}s_{inh}(t)(v - v_{inh}), \tag{2.2}$$

where  $v - v_{exc} < 0$  and  $v - v_{inh} > 0$  over the relevant range of  $v$ -values. The two terms in the sum represent effects of excitatory and inhibitory currents, respectively. We will assume that the synaptic variables  $s_{exc}(t)$  and  $s_{inh}(t)$  switch between values of 0 (off) and 1 (on) instantaneously and independently (Somers & Kopell, 1993; Othmer & Watanabe, 1994). This is a reasonable approximation in a situation where the input cells fire action potentials of stereotypical duration, sufficiently widely separated in time to allow for synaptic decay to a small level between inputs, and where the

synaptic onset and offset rates are rapid. We need not consider other aspects of the dynamics of the neurons supplying inputs to the model cell, as only the input timing will be relevant.

If the magnitude of  $I$  is not too large, then each of the four possible choices for  $(s_{exc}, s_{inh})$  yields a different  $v$ -nullcline of system 2.1, each of which has an  $N$ -like shape. For simplicity, we first consider the case  $s_{inh} = 0$ , so that the cell receives only excitatory input. We label the resulting nullclines as  $\mathcal{N}^i$ , with  $i \in \{E, 0\}$  corresponding to the values of  $s_{exc} = 1$  and  $s_{exc} = 0$ , respectively. The case when  $s_{inh} \neq 0$  can be treated similarly, resulting in two additional nullclines,  $\mathcal{N}^{I+E}$  and  $\mathcal{N}^I$ .

We refer to the left (right) branch of each  $v$ -nullcline  $\mathcal{N}^i$  as the *silent (active) phase*. Each left branch terminates where it coalesces with the middle branch in a saddle node bifurcation of equilibria for the  $v$ -equation. We denote these bifurcation points, or left knees, by  $(v_{LK}^i, w_{LK}^i)$ , and we denote the analogous right knees as  $(v_{RK}^i, w_{RK}^i)$ , with  $i \in \{E, 0\}$  as above. Since  $v - v_{exc} < 0$ , increasing  $s_{exc}$  lowers the  $v$ -nullcline in the  $(v, w)$  phase plane. See Figure 1 for an example of the arrangement of the nullclines and the different knees.

We have assumed that system 2.1 is excitable when excitation is off, with a stable critical point  $(v_{FP}^0, w_{FP}^0)$  on the left branch of  $\mathcal{N}^0$ . All solutions of equation 2.1 will therefore approach  $(v_{FP}^0, w_{FP}^0)$  in the absence of input. We assume that the critical point  $(v_{FP}^E, w_{FP}^E)$  lies on the middle branch of  $\mathcal{N}^E$ , so that the system is oscillatory in the presence of a constant excitatory input. This second assumption is not essential, and the analysis is easily generalized.

Note that in the singular limit, if  $w \in (w_{LK}^E, w_{FP}^0]$ , then an excitatory input results in a large excursion of  $v$ , corresponding to a spike. If excitatory inputs are brief, then any interesting dynamics is the consequence of synaptic inputs that result in such spikes. In remark 4, we comment further on the necessity of the assumptions made here.

**2.2 Timing of the Synaptic Inputs.** We denote the times at which the excitatory synaptic inputs occur by  $t_i$ , and we assume that each input has the same duration, which we call  $t^*$ . We will assume that  $t_{i+1} - t_i > t^*$ , so that the inputs do not overlap, and that the inputs are of equal strength, such that

$$s_{exc}(t) = \begin{cases} 1 & \text{if } t_i < t < t_i + t^*, \\ 0 & \text{otherwise.} \end{cases}$$

We comment on trains of inputs with variable durations and amplitudes in remarks 4 and 5.

Of fundamental interest in the following analysis will be the timing between subsequent excitatory inputs, which gives rise to the distribution of interexcitatory intervals  $T_i = t_{i+1} - t_i$ . We will assume that the  $T_i$  are

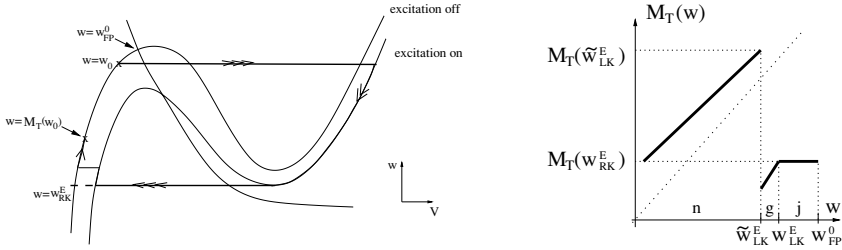


Figure 2: Schematic representation of a typical trajectory starting on the left branch of  $\mathcal{N}^0$  with  $w = w_0$ , where  $w_0$  is in the interval  $j = (w_{LK}^E, w_{FP}^0)$ , and ending on the same branch after time  $T$  (left).  $M_T(w_0)$  is defined as the  $w$  coordinate of the end point of the trajectory (right). Note that the trajectory from  $\tilde{w}_{LK}^E$  itself fails to reach the active phase, such that  $\tilde{w}_{LK}^E \cdot t^* = w_{LK}^E$  and  $M_T(\tilde{w}_{LK}^E) > w_{LK}^E$ .

independent and identically distributed random variables, with corresponding density  $\rho(t)$ . Excitation that is  $T$ -periodic in time is a special case, corresponding to the singular distribution  $\rho(t) = \delta(T)$ .

**2.3 Reduction of the Dynamics to a Map.** For the purposes of analysis, we consider that the active phase of the cell is very fast compared to the silent phase. More specifically, we treat the neuron as a three-timescale system. The first timescale, on the order of tenths of milliseconds, governs the evolution of the fast variable (the voltage) during spike onset and offset. The second, intermediate timescale, on the order of milliseconds, governs the evolution of the slow variable on the right-hand branch, while the third, slow timescale, on the order of tens of milliseconds, governs its evolution on the left-hand branch. We assume that the duration of excitation is greater than or equal to the duration of the active phase (Stuart & Häusser, 2001). Correspondingly, we measure input duration on the slowest timescale.

Using ideas of singular perturbation theory, these simplifications allow us to reduce the response of an excitable system to a one-dimensional map on the slow variable  $w$  in the singular limit. Similar maps have been introduced previously (Othmer & Watanabe, 1994), in the setting of two rather than three timescales. Since we measure the duration of excitation on the slow timescale, cells that spike are reinjected at  $w_{RK}^E$ , and the only accessible points on the left branch of  $\mathcal{N}^0$  lie in the interval  $I = [w_{RK}^E, w_{FP}^0]$  (see Figure 2).

A common dynamical systems convention is to denote the solution obtained by integrating a differential equation for time  $t$ , from initial condition  $x_0$ , by  $x_0 \cdot t$ . Using this convention, we denote the  $w$  coordinate at time  $t$ , of a point on the trajectory with initial condition  $(v_0, w_0)$ , by  $w_0 \cdot t$ . We now define a map  $M_T : I \rightarrow I$  by  $M_T(w_0) = w_0 \cdot T$ , where it is assumed that an excitatory input is received at time  $t = 0$ , at the start of the map cycle, and

no other excitatory inputs are received between times 0 and  $T$ . We claim that in the singular limit, there is no ambiguity in the definition of the map  $M_T$ . Indeed, in the singular limit, the initial point  $(v_0, w_0)$  can be assumed to lie on the left branch of the nullcline  $\mathcal{N}^0$ . Since the evolution on the right branch of  $\mathcal{N}^E$  occurs on the intermediate timescale and the time  $T$  exceeds the duration of excitation  $t^*$ , the trajectory starting at  $(v_0, w_0)$  again ends on the left branch of  $\mathcal{N}^0$  at time  $T$ . We emphasize that when we repeatedly iterate a map  $M_T$  or compose a sequence of maps  $M_{T_i}$ , we assume for consistency that an input arrives at the start of each map cycle and that no other inputs arrive during each cycle.

Figure 2 (left) shows a schematic depiction of part of a typical trajectory, starting on  $\mathcal{N}^0$  with  $w = w_0$ , during an interval of length  $T$  following an excitatory input. The trajectory jumps to the right nullcline after excitation is received. The jumps between the branches occur on the fast timescale (triple arrows), while the evolution on the right and left nullcline are intermediate and slow, respectively (double and single arrows). A possible form of the resulting map  $M_T$  is shown on the right. Note that this map has three branches. Let  $\tilde{w}_{LK}^E \leq w_{LK}^E$  denote the infimum of the set of  $w$ -values from which a cell will reach the active phase, when given an excitatory input of duration  $t^*$ . Orbits with initial conditions in the interval  $j = (w_{LK}^E, w_{FP}^0)$  will jump to the active phase as soon as excitation is received. Meanwhile, orbits with initial conditions in  $n = [w_{RK}^E, \tilde{w}_{LK}^E]$  will be blocked from reaching the active phase, by the left branch of the  $\mathcal{N}^E$  nullcline. Intermediate initial conditions, in  $g = (\tilde{w}_{LK}^E, w_{LK}^E]$ , will yield trajectories that jump to  $\mathcal{N}^E$  and then make a second jump, to the active phase, after a time  $0 \leq t < t^*$ . In the singular limit, the region  $j$  is compressed to a single point under  $M_T$ , so that  $M_T(j) = M_T(w_{RK}^E) = w_{RK}^E \cdot T$ . Since the times of entry into the active phase vary continuously across initial conditions in  $g$ ,  $M_T(g)$  has a nonzero slope. Finally, note that on  $n$ , the map  $M_T$  has slope less than one, corresponding to the fact that  $w'$  decreases as  $w$  approaches the fixed point  $w_{FP}^0$  along the left branch of  $\mathcal{N}^0$ .

**Remark 1.** The definition of the map  $M_T(w)$  can be extended to the case when the system is excitable rather than oscillatory under constant excitation, that is, when the point  $(v_{FP}^E, w_{FP}^E)$  is on the left branch of  $\mathcal{N}^E$ . In this case,  $M_T(w) < w$  may occur for  $w$  near  $w_{FP}^E$  if  $T$  is close to  $t^*$ , due to the stability of the fixed point  $(v_{FP}^E, w_{FP}^E)$  on  $\mathcal{N}^E$ .

**2.4 Periodic Excitation.** Although the case of periodic excitation has been analyzed in much detail elsewhere, we review it here since the analysis shares a common framework with the developments in the subsequent sections.

First, consider the limit as the duration of excitation goes to zero, with respect to the slow timescale, such that  $\tilde{w}_{LK}^E \uparrow w_{LK}^E$  and the middle branch

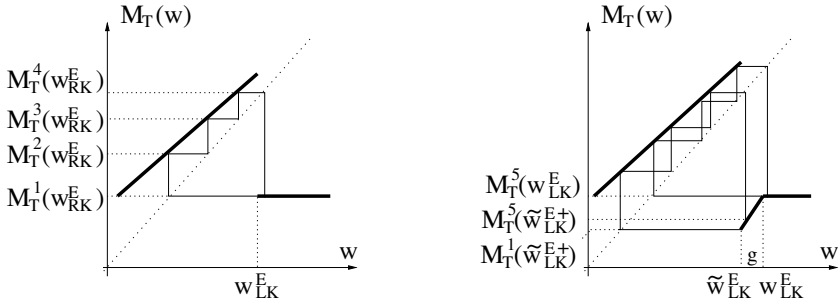


Figure 3: Examples of the map  $M_T$ . (Left) An example with  $t^* = 0$ , for which, after a finite number of iterations, all initial conditions will be mapped to a periodic orbit of period  $N = 4$ . (Right) An example with  $t^* > 0$ , with  $M_T^1(\tilde{w}_{LK}^{E+})$  defined as  $\lim_{w \downarrow \tilde{w}_{LK}^E} M_T^1(w)$ . This example exhibits contraction of the interval  $g$ , since  $M_T^5(g) \subset M_T^1(g)$  and  $|M_T^5(w_{LK}^E) - M_T^5(\tilde{w}_{LK}^{E+})| < |M_T^1(w_{LK}^E) - M_T^1(\tilde{w}_{LK}^{E+})|$ . Note that in both cases,  $M_T^1(w_{LK}^E) = M_T^5(w_{LK}^E)$ .

of  $M_T$  is eliminated. As shown in the left panel of Figure 3, the fact that  $j = (w_{LK}^E, w_{FP}^0)$  is contracted to a single point under  $M_T$  implies that all points  $w_0 \in I$  get mapped to a periodic orbit of  $M_T$  in a finite number of iterations. A simple analysis shows that there exists a natural number  $N$  such that a population of cells with initial conditions distributed on  $I$  will form  $N$  synchronous clusters under  $N$  applications of the map  $M_T$ . The periodic orbit is obtained from applying  $N$  iterations of  $M_T$  to  $M_T(w_{RK}^E)$ , and it consists of the points  $\{M_T^i(w_{RK}^E)\}_{i=1}^N$ , where  $M_T^N(w_{RK}^E) \in j$  (see Figure 3). Every trajectory is absorbed into this orbit, possibly after an initial transient. This clustered state persists away from the singular limit.

More precisely, consider the following intervals, or bins,

$$j_i = \left( M_T^{-i}(w_{LK}^E), M_T^{-(i-1)}(w_{LK}^E) \right] \quad i = 1, 2, \dots \tag{2.3}$$

Note that the  $i$ th iterate of  $j_i$  under  $M_T$  is contained in  $j$ . Therefore, since  $M_T^l(j_i) \subset j$ , it follows that  $M_T^{l+1}(j_i) = M_T(w_{RK}^E)$  or, more generally,  $M_T^l(j_i) = M_T^{-l+i}(w_{RK}^E)$  for  $l > i$ .

We can interpret this as follows. Consider a collection of identical oscillators subject to identical input, under the assumption that all oscillators have initial conditions in  $j_i$ . This collection will get mapped to the interval  $j$  just prior to the  $i$ th input. It will then respond to the  $i$ th input by firing in unison and will form a synchronous cluster after  $i + 1$  excitatory inputs, since the interval  $j$  collapses to a single point after the cells fire.

If the bin  $j_i$  contains a fraction  $q$  of the initial conditions, then this fraction of cells will fire at the  $i$ th input, as well as on every  $N$ th input after that.

Therefore, without knowing the distribution of initial conditions, it is not possible to know what fraction of the cell population will respond to a given input. Consider the two extreme examples: if all cells have initial conditions lying in one bin, the population of cells will respond only to every  $N$ th input. On the other hand, if initially every bin  $j_i$  contains some fraction of cells, then each input will induce a response by some fraction of the population.

Now consider the effect of  $t^* > 0$ , corresponding to a nonzero duration of excitation. As long as  $t^*$  is sufficiently small, or the slope of the middle branch of  $M_T$  is sufficiently shallow, then  $M_T$  will be contracting on  $g$ , as shown in the right panel of Figure 3. In this case, a similar clustered state arises away from the  $t^* = 0$  limit as well. Moreover, the definitions and clustering phenomenon described here carry over identically to the case of periodic excitation with inhibition held on at any constant level. In that case, the system will evolve on the nullclines  $\mathcal{N}^I$  and  $\mathcal{N}^{I+E}$  in the singular limit. The bins are defined in terms of the points  $w_{LK}^{I+E}$  and  $w_{RK}^{I+E}$ , rather than  $w_{LK}^E$  and  $w_{RK}^E$  as above.

We will show in the next section that under general conditions, the situation can be quite different when the times between onsets of successive excitatory inputs, which we will call interexcitation intervals (IEIs), are random and the possibility of sufficiently long IEIs exists.

**Remark 2.** The map  $M_T$  resembles a time  $T$  map of the voltage obtained from an integrate-and-fire system. In our case, the map is defined on the slow conductance  $w$ , however. If an excitatory input fails to elicit a spike and  $g(v, w)$  depends weakly on  $v$ , then the input may have little effect on the slow conductance. This is unlike the typical integrate-and-fire model, in which excitatory inputs move the cell closer to threshold.

### 3 The Construction of a Markov Chain

---

We next analyze the long-term statistical behavior of a cell that receives excitatory input that is not periodic in time. Our goals are to determine the probability that the cell fires in response to each subsequent input since it last fired and the number of inputs the cell is expected to receive between firings or, equivalently, the average number of failures before a spike occurs. Our results can be interpreted in the context of a population of cells as well, and this is discussed in section 5.

A key point in our approach is that, as noted in section 2, all firing events lead to reinjection at  $w_{RK}^E$ . Therefore, the system has only limited memory, since after a cell fires, all information about its prior behavior is erased. This allows us to describe the evolution of the variable  $w$  through the interval  $[w_{RK}^E, w_{FP}^0]$  as a Markov process with a finite number of states. The steps in this process will be demarcated by the arrival times of excitatory inputs. Each IEI is defined as the time from the onset of one excitatory input to the

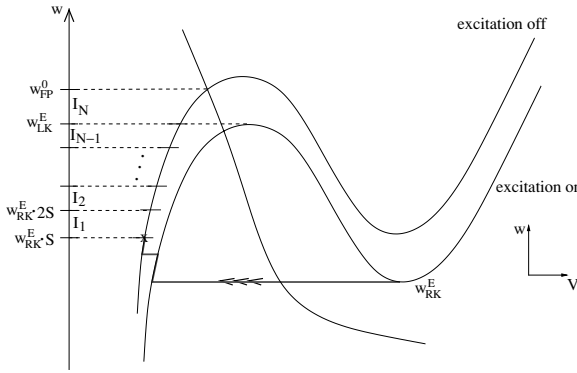


Figure 4: Bins  $I_j$  are defined by intervals of values of the slow variable  $w$ . Note that larger subscripts label intervals of larger  $w$  values. Iterations of  $w_{RK}^E$  for integer multiples of the minimal IEI time  $S$  are used to define most bins, as in equation 3.1, whereas bins  $I_{N-1}$  and  $I_N$  are defined using  $w_{LK}^E$  and  $w_{FP}^0$ , as in equation 3.2.

onset of the next. The length of this interval includes the duration of the input that occurs at the start of the IEI.

We assume that the lengths of the IEIs, which we denote by  $T$ , are independent and identically distributed random variables with density  $\rho$ . Fundamental in our analysis is the assumption that the support of  $\rho$  takes the form  $[S, U]$ , where  $0 < S < U < \infty$ . As long as the frequency of the cells providing excitatory inputs is bounded, this assumption is not unreasonable. If  $\rho$  satisfies this assumption, then the long-term behavior of a population of cells is accurately captured by the asymptotics of a corresponding Markov chain with finitely many states. We show that under certain conditions, this Markov chain is aperiodic and irreducible and thus has a limiting distribution. This distribution can be used to describe the firing statistics of the cell.

**3.1 The States of the Markov Chain.** We start by again assuming that the cell receives only excitatory input. To simplify the exposition, we now assume that the input is instantaneous on the slow timescale, so that it causes a cell to spike if and only if  $w > w_{LK}^E$ . In the singular limit, such an input has no effect on the slow variable  $w$  of a cell unless a spike is evoked. This assumption will be relaxed subsequently.

In the case of periodic excitation, we considered bins defined by backward iterations of  $w_{LK}^E$ , as in equation 2.3. For notational reasons, it is now more convenient to consider forward iterations of  $w_{RK}^E$  to form bins used in the definition of the Markov chain (see Figure 4). Let  $N$  be the smallest number such that  $w_{RK}^E \cdot NS > w_{LK}^E$ , where  $S > 0$  is the lower bound of

the support of  $\rho$  mentioned above. Therefore,  $N$  is the maximal number of excitatory inputs that a cell starting at any point  $w_0 \in [w_{RK}^E, w_{FP}^0]$  can receive before firing. Set

$$I_k = [w_{RK}^E \cdot kS, w_{RK}^E \cdot (k+1)S] \quad \text{if} \quad 1 \leq k \leq N-2, \quad (3.1)$$

and define two additional bins:

$$\begin{aligned} I_{N-1} &= [w_{RK}^E \cdot (N-1)S, w_{LK}^E] \\ I_N &= (w_{LK}^E, w_{FP}^0) = j. \end{aligned} \quad (3.2)$$

If  $T$  is a random variable, then the map  $M_T$  transfers ensembles of cells between bins. This process is non-Markovian, in that transition probabilities depend on the full set of IEIs that have occurred since a cell last spiked, and not just current bin membership. That is, a cell that enters a bin after fewer inputs will be more likely to lie in the lower part of the bin than a cell that enters the same bin after more inputs. Hence, the number of inputs that a cell has received since its last spike can significantly affect its transition probabilities between bins. Therefore, to form a Markov chain from  $M_T$ , a further refinement is needed. To that effect, we define Markov chain states  $(I_k, l)$  as follows. A cell is in state  $(I_k, l)$  if  $w \in I_k$  and  $l$  complete IEIs have passed since the cell last fired. Note that by construction, the first of these IEIs ( $l = 1$ ) actually corresponds to the duration of the input that made the cell fire, together with the pause between that input and the next, since the actual firing and reset occur relative to the slow timescale.

As in the case of periodic excitation, the analysis carries over directly to the case of constant inhibition. In this case, the nullclines  $\mathcal{N}^I$  and  $\mathcal{N}^{I+E}$  are used instead of  $\mathcal{N}^0$  and  $\mathcal{N}^E$  above. The remainder of the above construction is identical, with the superscripts  $I$  and  $I + E$  replacing the superscripts  $0$  and  $E$ , respectively.

**Remark 3.** For the remainder of this section, we continue to denote the states of the Markov chain by  $(I_k, l)$ , to emphasize that the first index refers to an interval of slow variable values. For simplicity, we use  $(k, l)$  instead of  $(I_k, l)$  in the examples of the analysis that appear later in the letter.

**Remark 4.** Up to this point, we have made several assumptions that can in fact be weakened in the following ways:

- For  $\varepsilon \neq 0$ , the actual jump-up threshold lies below  $w_{LK}^E$  and is given by the minimal level of  $w$  for which an input current pushes the point  $(v, w)$  on the left branch of  $\mathcal{N}^0$  into the active phase. As long as all inputs are the same (otherwise, see the next point and remark 5), this value is uniquely defined and can be used to replace  $w_{LK}^E$  in the definitions of  $I_{N-1}$  and  $I_N$  in equation 3.2.

- If the excitatory input is not instantaneous in time, then the bins have to be adjusted. For instance, the top bin will include all cells that fire by jumping to the left branch of  $\mathcal{N}^E$  and then reaching  $w_{LK}^E$  with the input still on. Each IEI will consist of the duration of the excitatory input beyond reset (see the next point), plus the time until the arrival of the next input. The distribution of IEIs must be adjusted accordingly. These steps are incorporated in the examples presented in section 6.
- As stated in section 2, when inputs are not instantaneous, input duration is measured on the slowest timescale. It is possible, however, that the input duration, in milliseconds, is only slightly longer than the active phase, which transpires on our intermediate timescale. What we refer to here as the input duration is therefore really the duration of the part of the input that extends beyond the cell's return to the silent phase, which we measure on the slow timescale.
- If the input turns on and off gradually, then the analysis becomes more complicated, although additional simplifying assumptions could reduce this complexity.

**3.2 Transition Probabilities.** To complete the definition of the Markov chain, we need to compute the transition probabilities between the different states. The transitions occur at times at which the cell receives excitatory inputs. One way to think about this probability is to imagine a large pool of noninteracting cells, each of which receives a different train of inputs with IEIs chosen from the same distribution. To start, assume that each cell is in bin  $I_N$  and receives its next excitatory input at slow time 0. By the definition of  $I_N$ , these inputs cause the cells to spike, and they get reinjected at  $w_{RK}^E$ , still at slow time 0. The assumption that all cells are reset to the same point is essential in the definition of the Markov chain.

Recall that we have defined the length  $T$  of an IEI as the time between the onsets of two subsequent inputs and that these times are independent and drawn from the distribution  $\rho$ . Focus on a particular cell, and denote the length of its next IEI by  $T_1$ . Just before the cell's next input arrives, it will be at  $w_{RK}^E \cdot T_1$ . Similarly, if we check the locations of all other cells after their respective IEIs, we will find that the population of cells is distributed in some interval starting at  $w_{RK}^E \cdot S$ , as shown in Figure 5. The transition probability from the state  $(I_N, k)$  to the state  $(I_j, 1)$  equals the fraction of the population of cells that are in bin  $I_j$  at the ends of their respective IEIs. This fraction is independent of the number of inputs  $k$  a cell received before firing, by our assumption that all information about prior dynamics is erased once a cell has fired.

Let us return to the cell at  $w_{RK}^E \cdot T_1$ , and let  $T_2$  denote its second IEI since time 0, also chosen from the distribution  $\rho$ . After this IEI, the example cell will be at  $w_{RK}^E \cdot (T_1 + T_2)$ . The fraction of the population lying in bin  $I_j$  after one IEI since time 0 and in bin  $I_k$  after two IEIs since time 0 is

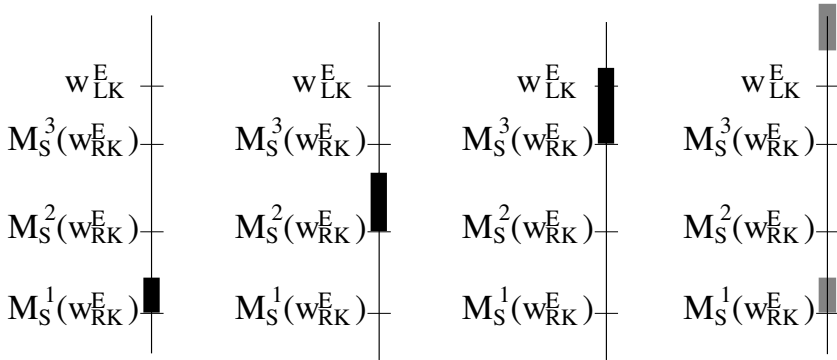


Figure 5: An example of the state of the population of cells that start in  $I_N$  and immediately receive inputs and fire. After one subsequent IEI, the cells are at  $w_{RK}^E \cdot T$ , where  $T$  is distributed according to  $\rho$ . Therefore, all cells lie in an interval bounded below by  $M_S^1(w_{RK}^E) = w_{RK}^E \cdot S$ , as shown in the left-most part of the figure. For this example, we have assumed that  $\text{supp}(\rho) \subset [S, 2S)$ , such that all cells are below  $M_S^2(w_{RK}^E) = w_{RK}^E \cdot 2S$ , as shown. After a second IEI, each cell is at  $w_{RK}^E \cdot (T_1 + T_2)$ , where both  $T_1$  and  $T_2$  are chosen from the distribution  $\rho$ . After a third IEI, some cells will lie above  $w_{LK}^E$ , such that they fire to their next inputs, while others will not. The distributions of cells after the third and fourth IEIs are the right-most two distributions shown above.

the transition probability between the states  $(I_j, 1)$  and  $(I_k, 2)$ . This process can be continued to compute all the transition probabilities. In the example shown in Figure 5, we have assumed that  $\text{supp}(\rho) \subset [S, 2S)$  and that there are five accessible states, which we order as  $(I_1, 1)$ ,  $(I_2, 2)$ ,  $(I_3, 3)$ ,  $(I_4, 3)$ , and  $(I_4, 4)$ . Hence,  $N = 4$ , and the matrix of transition probabilities has the form

$$A = \begin{bmatrix} 0 & 1 & 0 & 0 & 0 \\ 0 & 0 & * & * & 0 \\ 0 & 0 & 0 & 0 & 1 \\ 1 & 0 & 0 & 0 & 0 \\ 1 & 0 & 0 & 0 & 0 \end{bmatrix}, \tag{3.3}$$

where  $A_{ij}$  gives the transition probability from the  $i$ th state in the list to the  $j$ th state in the list.

If initial conditions are selected randomly, then some cells may initially lie in transient states that cannot be reached subsequent to reset from  $w_{RK}^E$ . We neglect such states in the Markov chain, since including them does not affect the statistics we consider.

We now are ready to compute the transition probabilities for the general Markov chain that we have defined. We first compute transition

probabilities between the states  $(I_j, l)$  and  $(I_k, l + 1)$  for  $l \leq j < k \leq N$ . Consider independent and identically distributed random variables  $T_i$ , each with probability density  $\rho$ . Let  $\sigma_l = \sum_{i=1}^l T_i$  denote the sum of these random variables. The transition probability between the states  $(I_j, l)$  and  $(I_k, l + 1)$  is given by

$$\begin{aligned} p_{(j,l) \rightarrow (k,l+1)} &= P[(I_k, l + 1) | (I_j, l)] \\ &= P[\sigma_{l+1} \in [kS, (k + 1)S] \mid \sigma_l \in [jS, (j + 1)S)]. \end{aligned} \tag{3.4}$$

Since the probability density  $\rho^{(l)}$  of the sum  $\sigma_l$  can be computed recursively by the convolution formula,

$$\rho^{(l)}(t) = \int \rho^{(l-1)}(u)\rho(t - u)du,$$

the conditional probabilities in the expression above can be evaluated. In particular, since

$$P[\sigma_{l+1} \in [z, z + \Delta z] \ \& \ \sigma_l \in [w, w + \Delta w]] \approx \rho^{(l)}(w)\rho(z - w)\Delta w \Delta z,$$

it follows that

$$p_{(j,l) \rightarrow (k,l+1)} = \frac{\int_{kS}^{(k+1)S} \int_{jS}^{(j+1)S} \rho^{(l)}(w)\rho(z - w)dw dz}{\int_{jS}^{(j+1)S} \rho^{(l)}(z)dz}. \tag{3.5}$$

Next, we define the transition probabilities from the states  $(I_N, l)$ . By our assumption, a cell in one of these states fires when it receives an excitatory input. Therefore, the next state must be of the form  $(I_j, 1)$ . As discussed above, once a cell fires, it has no memory of the number of excitatory inputs it received prior to this event. Therefore, the transition probability from  $(I_N, l)$  to  $(I_j, 1)$  is the same for all  $l$ . This transition probability can be obtained as

$$p_{(N,l) \rightarrow (j,1)} = P[(I_j, 1) | (I_N, l)] = \int_{jS}^{(j+1)S} \rho(t)dt.$$

Since no transitions other than the ones described above are possible, this completes the definition of the Markov chain. As a final step, let  $I_{k_i}$  denote the highest bin, with respect to values of the slow variable, that can be reached through  $i$  IEIs after reset. To form the transition matrix  $A$  for the Markov chain, we simply order the states of the Markov chain in the list

$$(I_1, 1), (I_2, 1), \dots, (I_{k_1}, 1), (I_2, 2), (I_3, 2), \dots, (I_{k_2}, 2), \dots, (I_N, N).$$

The transition from the  $m$ th state to the  $n$ th state in the list is taken to be the  $(m, n)$  element of the matrix  $A$ , as was done in matrix 3.3 in the above example.

**Remark 5.** As mentioned in remark 4, the threshold  $w_{LK}^E$  in equation 3.2 depends on input amplitude and duration. If input amplitudes are not constant, then there will no longer be a single value  $N$  such that a cell fires to its next input if and only if it is in a state of the form  $(I_N, j)$ , no matter how  $I_N$  is defined. In such a case, we can, for example, use the threshold defined for the maximal relevant input amplitude to define  $I_N$ . Then the probability distribution of input amplitudes can be used to compute probabilities  $p_{(N,l) \rightarrow (N,l+1)}$  and  $p_{(N,l) \rightarrow (j,1)}$ . For some range of  $l$  values,  $p_{(N,l) \rightarrow (N,l+1)}$  will be nonzero, and there will be a maximal value  $l$  such that no cell requires more than  $l$  inputs to fire, and hence  $(I_N, l)$  is the last state in the chain.

#### 4 Limiting Distributions of the Markov Chain and Their Interpretation

We next consider the long-term behavior of the Markov chains defined above and interpret this behavior in terms of the original fast-slow system. For a finite-state Markov chain with  $M$  states and transition matrix  $A$ , the probability distribution  $\pi = (\pi_1, \dots, \pi_M)$  is a stationary distribution if  $\sum_i \pi_i A_{i,j} = \pi_j$  for all  $j$ . The stationary distribution  $\pi$  is a limiting distribution if

$$\lim_{n \rightarrow \infty} \{A^n\}_{i,j} = \pi_j.$$

A Markov chain is irreducible if for any two states  $i$  and  $j$ , there exists a finite  $n$  such that  $\{A^n\}_{i,j} > 0$ . In other words, there is a nonzero probability of transition between any two states in a finite number of steps. An irreducible finite state Markov chain has a unique stationary distribution (Hoel, Port, & Stone, 1972). The period  $d_i$  of the state  $i$  in a Markov chain is the greatest common divisor of the set  $\{n | \{A^n\}_{i,i} > 0\}$ . For an irreducible chain, all states have the same period  $d$ . Such a chain is called aperiodic if  $d = 1$  and periodic if  $d > 1$ . A key point is made in the following theorem:

**Theorem 1** ((Hoel et al., 1972), p. 73). *For an aperiodic, irreducible Markov chain, the stationary distribution is a limiting distribution.*

**4.1 Conditions for the Existence of a Limiting Distribution.** We next show that under very general conditions, the Markov chain constructed in the previous section is irreducible and aperiodic and therefore has a limiting distribution. First, recall that the chain was constructed to include precisely those states that can be reached with nonzero probability in a finite number of steps after a cell is reset. Since a cell in any state will fire and

be reset after a finite number of steps, this implies that there is a nonzero probability of transition from any state to any other state in the chain in a finite number of steps. Therefore, the Markov chain under consideration is always irreducible.

We next consider conditions under which the Markov chain is aperiodic. It is sufficient to start with a continuum ensemble of cells at  $w_{RK}^E$ . If these cells are subject to different realizations of the input, and a nonzero fraction of cells occupies every state after a finite number inputs, then the transition matrix is aperiodic.

To start, note that if  $\rho$  is supported on a single point  $T$ , so that the input is periodic, then the Markov chain will be periodic. Each point  $M_T^i(w_{RK}^E)$  is contained in bin  $I_j$ . Therefore the states of the Markov chain are  $\{(I_i, i)\}_{i=1}^N$ . In the case depicted in Figure 3, for example, the transition matrix has the form

$$A = \begin{bmatrix} 0 & 1 & 0 & 0 \\ 0 & 0 & 1 & 0 \\ 0 & 0 & 0 & 1 \\ 1 & 0 & 0 & 0 \end{bmatrix}. \tag{4.1}$$

Consider next what happens as the support of  $\rho$  is enlarged to  $[T, T + \delta]$  in this example. For small  $\delta$ , there is no change in the structure of the transition matrix. For some  $\delta_0$  sufficiently large, however, we have  $M_{3(T+\delta_0)}(w_{RK}^E) = w_{LK}^E$ , and when  $\delta > \delta_0$ , as shown in Figure 5, a fraction of the cells will be in state  $(I_3, 3)$  after three IEIs, while another fraction will be in state  $(I_4, 3)$ . When their next excitatory input arrives, the cells in state  $(I_4, 3)$  will fire and transition to  $(I_1, 1)$ , whereas the cells in  $(I_3, 3)$  will require two more inputs to fire. Therefore, in addition to the states  $(I_1, 1), (I_2, 2), (I_3, 3), (I_4, 4)$  that were relevant in the periodic case, the new state  $(I_4, 3)$  becomes part of the Markov chain. The transition matrix between these five states for  $\delta > \delta_0$  has the form

$$A = \begin{bmatrix} 0 & 1 & 0 & 0 & 0 \\ 0 & 0 & 1 - \varepsilon(\delta) & \varepsilon(\delta) & 0 \\ 0 & 0 & 0 & 0 & 1 \\ 1 & 0 & 0 & 0 & 0 \\ 1 & 0 & 0 & 0 & 0 \end{bmatrix}, \tag{4.2}$$

where  $\varepsilon(\delta_0) = 0$ ,  $\varepsilon$  increases with  $\delta$ , and the states are ordered as  $(I_1, 1), (I_2, 2), (I_3, 3), (I_4, 3),$  and  $(I_4, 4)$ . It can be checked directly that this transition matrix is aperiodic. This is also a consequence of the following general theorem:

**Theorem 2.** *Suppose that the support of the distribution  $\rho$  of IEIs (including input durations) is the interval  $[S, U]$ . The transition matrix defined in section 3*

is aperiodic if and only if  $M_{iU}(w_{RK}^E) > w_{LK}^E$  for an integer  $0 < i < N$ , where  $N$  is defined by  $M_{(N-1)S}(w_{RK}^E) < w_{LK}^E < M_{NS}(w_{RK}^E)$ , as in section 3.

**Corollary 1.** *The Markov chain defined above has a limiting distribution if and only if  $M_{iU}(w_{RK}^E) > w_{LK}^E$  for an integer  $0 < i < N$ , where  $N$  is described in theorem 2.*

**Remark 6.** In the example discussed above, as the support of  $\rho$  widens, the periodic transition matrix in equation 4.1 is replaced by the aperiodic matrix, equation 4.2. Since the limiting behavior of periodic and aperiodic Markov chains is very different, the system can be thought of as undergoing a bifurcation as  $\delta$  is increased past  $\delta_0$ .

**Proof.** If  $M_{iU}(w_{RK}^E) \leq w_{LK}^E$  for all integers  $0 < i < N$ , then it can be checked directly that the only states that are achievable from an initial condition  $M_S(w_{RK}^E)$  have the form  $(I_i, i)$  for  $0 < i \leq N$ . Therefore, the transition matrix is of size  $N \times N$  and has the form of matrix 4.1, with ones on the superdiagonal in all rows except the last, which has a one in its first column. Thus, the Markov chain is periodic.

Assume instead that  $M_{iU}(w_{RK}^E) > w_{LK}^E$  for an integer  $0 < i < N$ . Consider a continuum of cells that have just spiked and been reset to  $w_{RK}^E$  and are receiving independent realizations of the input. First, note that after  $i$  IEIs following the spike, there will be a nonzero fraction of cells in all states  $(I_k, i)$ ,  $k \geq i$  that are part of the Markov chain.

The condition  $M_{iU}(w_{RK}^E) > w_{LK}^E$  and the fact that the support of  $\rho$  is an interval imply that some cells will fire on the  $i$ th,  $(i + 1)$ st,  $\dots$ , and  $N$ th inputs after the one that causes their initial reset. Correspondingly, there will be cells in all states  $(I_k, 1)$ ,  $k \geq 1$  in the chain after the  $i$ th input, cells in all states  $(I_k, 2)$ ,  $k \geq 2$  and  $(I_k, 1)$ ,  $k \geq 1$  in the chain after the  $(i + 1)$ st input, and so on, until all states of the form  $(I_k, j)$  with  $k \geq j$  and  $j \in \{1, \dots, N - i + 1\}$  are nonempty after  $N$  inputs. Similarly, some cells will fire again to input number  $2i$ , with some other cells firing to each input from  $2i + 1$  up to  $2N$ , and after  $2N$  inputs, all states  $(I_k, j)$  with  $k \geq j$  and  $j \in \{1, \dots, 2N - 2i + 1\}$  in the chain will be nonempty. Continuing this argument inductively shows that all states are necessarily occupied just before the arrival of the  $(bN)$ th input after reset (i.e., after  $bN$  IEIs), where  $b = \lceil \frac{N-1}{N-i} \rceil$ —namely, the least integer greater than or equal to  $(N - 1)/(N - i)$ , such that  $bN$  is bounded above by  $(N - 1)N$ , since  $i \leq N - 1$ . This establishes theorem 2.

Finally, since we established previously that the Markov chain is irreducible, theorems 1 and 2 imply that it has a limiting distribution whenever  $M_{iU}(w_{RK}^E) > w_{LK}^E$  for an integer  $0 < i < N$ . If this condition fails, then the Markov chain is periodic and therefore has no limiting distribution. Hence, corollary 1 holds as well.

**4.2 Interpretation of the Invariant Density.** The limiting distribution  $Q$  of the derived Markov chain has two interpretations (Taylor & Karlin, 1998). Assume that a cell is subjected to excitatory input for a long time. If  $w$  is recorded after each IEI, just prior to the moment when the cell receives an excitatory input, then  $Q[(I_j, l)]$  is the fraction of recordings observed to fall inside  $(I_j, l)$ . Consequently, the total mass of the distribution  $Q$  that lies in the states  $(I_N, j)$ , namely,  $\sum_{j=1}^N Q[(I_N, j)]$ , is the probability that a cell will respond to the next excitatory input by firing. Similarly, we can think of  $Q[(I_j, l)] / \sum_{k=l}^N Q[(I_k, l)]$  as the probability that a cell will be found to have  $w \in I_j$  just prior to receiving its  $l$ th excitatory input since it fired last.

Note that the firing probability  $\sum_{j=1}^N Q[(I_N, j)]$  is not the reciprocal of the average number of failures before a spike. However, the average number of failures, call it  $E_f$ , can be computed once the  $Q[(I_j, l)]$  are known. Clearly,

$$E_f = \sum_{j=1}^{N-1} jF_j, \tag{4.3}$$

where each  $F_j$  denotes the probability that exactly  $j$  failures occur. Note that  $j$  failures occur precisely when  $j + 1$  conditions are met. That is, for each  $i = 1, \dots, j$ , just prior to the  $i$ th input since the last firing, the trajectory falls into a state of the form  $(I_k, i)$ , where  $i \leq k_i < N$ . Further, the trajectory ends in state  $(I_N, j + 1)$  before the  $(j + 1)$ st input, to which the cell responds by firing. The quantity

$$\frac{\sum_{k=i}^{N-1} Q(I_k, i)}{\sum_{k=i}^N Q(I_k, i)}$$

equals the probability that just before the  $i$ th input arrives, a cell will lie in a state  $(I_k, i)$  with  $k < N$ . Thus, the failure probabilities are given by

$$F_j = \left( \frac{\sum_{k=1}^{N-1} Q(I_k, 1)}{\sum_{k=1}^N Q(I_k, 1)} \right) \left( \frac{\sum_{k=2}^{N-1} Q(I_k, 2)}{\sum_{k=2}^N Q(I_k, 2)} \right) \dots \left( \frac{\sum_{k=j}^{N-1} Q(I_k, j)}{\sum_{k=j}^N Q(I_k, j)} \right) \left( \frac{Q(I_N, j + 1)}{\sum_{k=j+1}^N Q(I_k, j + 1)} \right). \tag{4.4}$$

Of course, while some of the  $Q(I_k, j)$  may be zero, the exclusion of transient states in our Markov chain construction ensures that all of the sums in the denominators of equation 4.4 will be positive for every population of cells.

Finally, we note that the eigenvalues of the transition matrix can be used to quantify the rate at which the system will converge to its limiting distribution, when one exists. This information may be useful even if Monte Carlo simulations will be used.

## 5 Extensions of the Markov Chain Approach

---

The ideas introduced in the previous section are applicable in many other settings. Here we outline extensions to heterogeneous populations of excitable cells subject to identical periodic input and to general excitable systems and related models.

**5.1 Populations and Heterogeneity.** The limiting distribution computed from a Markov chain cannot be used directly to determine what fraction of a population of identical cells subject to identical stochastic trains of excitatory inputs will respond to a given input. As noted earlier, it is necessary to specify the distribution of initial conditions to compute this fraction. On the other hand, the limiting distribution contains information about a population of identical cells subject to different realizations of the stochastic train of excitatory inputs (Taylor & Karlin, 1998). In this case, all of the quantities discussed in the previous section can be reinterpreted with respect to the firing statistics of a population of cells. For example, the fraction of cells responding with a spike to a given excitatory input equals the probability of a single cell firing to a particular excitatory input, that is,  $\sum_{j=1}^N Q[(I_N, j)]$ .

We can also apply similar ideas to the case of a heterogeneous population of excitable cells all subject to the same periodic input, say, of period  $T$ . Heterogeneity in intrinsic dynamics may lead to different rates of evolution for different cells in the silent phase, but this disparity can be eliminated by rescaling time separately for each cell, so that all cells evolve at the same unit speed in the silent phase. As a result of this rescaling, the heterogeneity in the population will become a heterogeneity in firing thresholds. Denote the resulting distribution of thresholds by  $\phi$ , such that for any  $t > 0$ ,  $\int_0^t \phi(\tau) d\tau$  gives the fraction of cells with thresholds below  $t$ . There will exist a maximal nonnegative integer  $m$  and a minimal positive integer  $n > m$  such that the support of the distribution  $\phi$  is contained in the interval  $[mT, nT]$ . Thus, for  $i \geq 1$ ,  $\delta_i = \int_{(i-1)T}^{iT} \phi(\tau) d\tau$  gives the fraction of cells that will fire in response to the  $i$ th input, which is nonzero for  $i = m + 1, \dots, n$ .

We can define Markov chain states  $I_j$ , for  $j = 1, \dots, n$ , by stating that a cell is in state  $I_j$  if it has received  $j - 1$  inputs since it last fired. The transition probability  $P(j, j + 1)$  from state  $I_j$  to state  $I_{j+1}$  is 1 if  $j \leq m$ ; if  $j = m + 1$ , then  $P(m + 1, m + 2) = 1 - \delta_{m+1}$ , while the probability of transition from state  $I_m$  to state  $I_1$  is  $P(m + 1, 1) = \delta_{m+1}$ ; and if  $m + 1 < j \leq n - 1$ , then  $P(j, j + 1)$  is given by the proportion of those cells that have not fired to

the first  $j - 1$  inputs that also do not fire to the  $j$ th input, namely,

$$\begin{aligned}
 P(j, j + 1) &= 1 - \gamma_j := \frac{1 - \delta_j - \delta_{j-1} - \dots - \delta_{m+1}}{1 - \delta_{j-1} - \delta_{j-2} - \dots - \delta_{m+1}} \\
 &= 1 - \frac{\delta_j}{1 - \delta_{j-1} - \delta_{j-2} - \dots - \delta_{m+1}},
 \end{aligned}$$

while  $P(j, 1) = \gamma_j = \delta_j / (1 - \delta_{j-1} - \dots - \delta_{m+1})$ . Finally, the transition probability from state  $I_n$  to state  $I_1$  is 1, and all other transitions have zero probability. If we set  $\gamma_{m+1} = \delta_{m+1}$ , then the transition matrix takes the form

$$A = \begin{bmatrix}
 0 & 1 & 0 & 0 & \dots & 0 & 0 & \dots & 0 & 0 \\
 0 & 0 & 1 & 0 & \dots & 0 & 0 & \dots & 0 & 0 \\
 \cdot & \cdot & \cdot & \cdot & \dots & \cdot & \cdot & \dots & \cdot & \cdot \\
 \cdot & \cdot & \cdot & \cdot & \dots & \cdot & \cdot & \dots & \cdot & \cdot \\
 \cdot & \cdot & \cdot & \cdot & \dots & \cdot & \cdot & \dots & \cdot & \cdot \\
 \gamma_{m+1} & 0 & 0 & 0 & \dots & 1 - \gamma_{m+1} & 0 & \dots & 0 & 0 \\
 \cdot & \cdot & \cdot & \cdot & \dots & \cdot & \cdot & \dots & \cdot & \cdot \\
 \cdot & \cdot & \cdot & \cdot & \dots & \cdot & \cdot & \dots & \cdot & \cdot \\
 \cdot & \cdot & \cdot & \cdot & \dots & \cdot & \cdot & \dots & \cdot & \cdot \\
 \gamma_{n-1} & 0 & 0 & 0 & \dots & 0 & 0 & \dots & 0 & 1 - \gamma_{n-1} \\
 1 & 0 & 0 & 0 & \dots & 0 & 0 & \dots & 0 & 0
 \end{bmatrix}.$$

As long as  $m < n - 1$ , such that the distribution  $\phi$  has support on an interval of length greater than  $T$ , not all cells will fire together. Under this condition, there exists  $i < n$  such that  $\delta_i \neq 0$  and, correspondingly,  $\gamma_i \neq 0$ . In this case, the proof of theorem 2 immediately generalizes to show that there exists a sufficiently large number of iterations  $N$  such that  $\{A^r\}_{i,i} > 0$  for all  $r > N$ , which implies that  $A$  is aperiodic and the Markov chain has a limiting distribution.

This result can be interpreted as follows. If the heterogeneity is weak, then cells starting with the same initial condition will always respond to the same inputs in a train, giving an unreliable population response. With a stronger degree of heterogeneity, the population response will disperse, eventually every input will evoke a response from some nonempty subset of the cells, and the statistics of the population response will be given by the limiting distribution of the Markov chain.

**5.2 General Excitable Systems and Related Models.** An excitable system can be characterized by the existence of a stable rest state and a threshold. In such a system, when a perturbation pushes a trajectory from the rest state across the threshold, the trajectory makes a significant excursion before returning to a small neighborhood of the rest state. Suppose that an  $n$ -dimensional excitable system receives transient inputs of a stereotyped

form. If we select a time  $T$ , then we can define a map  $M_T(u)$  having as its domain a set of starting states  $u$  for the system, each of which is an  $n$ -dimensional vector.

In theory, bins in  $n$ -dimensional space could be defined to implement the Markov chain approach for an  $n$ -dimensional map. Indexing these bins efficiently and computing transition probabilities between them could become problematic when  $n$  is not small, however. On the other hand, the Markov chain approach discussed in the previous section can be applied directly to systems for which  $M_T(u) = u(T)$  lie (approximately) on an interval in the phase space of the system, and which are reset to a fixed value  $u_{reset}$  after crossing threshold. The assorted versions of the integrate-and-fire (IF) model (leaky IF, quadratic IF, exponential IF, and so on) in the subthreshold regime satisfy both of these conditions, as do the lighthouse model of (Haken, 2002; Chow & Coombes, 2006) and the Kuramoto (1984) model on  $S^1$ . There is an important difference between the excitable systems considered in detail here and the IF model, however. When the results derived for excitable systems are applied to neuronal models, the Markov chain will be defined using a slowly changing ionic conductance, or an associated activation or inactivation, while in the case of the IF model, it would be defined in terms of the voltage. As a consequence, for the IF case, one would need to take into account the jumps in voltage due to synaptic inputs when defining the states of the Markov chain and computing the transition probabilities. Moreover, an additional difficulty arises from the fact that voltage will decrease after the application of an input that pulls the model above its intrinsic rest state but fails to cause a threshold crossing. This nonmonotonicity will complicate bin definitions. A similar issue will arise even in an excitable system with one slow variable  $w$  if the system remains excitable while its input is on. In this case,  $w$  converges toward  $w_{FP}^E$  whenever  $w \in (w_{FP}^E, w_{LK}^E)$  on  $\mathcal{N}^E$ .

## 6 An Example: The TC Model

---

A prototypical representative of the class of models to which the analysis outlined in the preceding sections is applicable is a model for a thalamocortical relay (TC) cell relevant for the study of Parkinson's disease (PD) and deep brain stimulation (DBS). The TC model that we consider takes a similar form to the reduced TC model in Rubin and Terman (2004):

$$\begin{aligned} C_m v' &= -I_L - I_T - g_{exc} s_{exc}(v - v_{exc}) - g_{inh} s_{inh}(v - v_{inh}) \\ w' &= \phi(w_\infty(v) - w)/\tau(v). \end{aligned} \tag{6.1}$$

Here, the leak current  $I_L = g_L(v - v_L)$  and the T-type or low-threshold calcium current  $I_T = g_T m_\infty(v)w(v - v_{Ca})$ , with parameter values  $C_m = 1 \mu\text{F}/\text{cm}^2$ ,  $g_L = 1.5 \text{ mS}/\text{cm}^2$ ,  $v_L = -68 \text{ mV}$ ,  $g_T = 5 \text{ mS}/\text{cm}^2$ ,  $v_{Ca} = 90 \text{ mV}$ ,

$g_{exc} = 0.08$  mS/cm<sup>2</sup>,  $v_{exc} = 0$  mV,  $g_{inh} = 0.12$  mS/cm<sup>2</sup>,  $v_{inh} = -85$  mV,  $\phi = 3.5$  and functions  $m_\infty(v) = (1 + \exp(-(v + 35)/7.4))^{-1}$ ,  $w_\infty(v) = (1 + \exp((v + 61)/9))^{-1}$ , and  $\tau(v) = 10 + 400/(1 + \exp((v + 50)/3))$ . The values of  $s_{exc}$  and  $s_{inh}$  will be determined by stochastic processes discussed below, and we made an additional modification to the model to make it oscillatory in the presence of excitation, which is discussed in remark 8. The assumptions that we make regarding the presence of three timescales in the dynamics are not unreasonable in this model, as shown in Rubin and Terman (2004) and Stone (2004).

In this section, we present the analytical results of the Markov chain approach for this model for two particular IEI distributions, one uniform and one normal, both with inhibition held off for all time and with inhibition held on for all time (further details appear in appendixes A and B). We compare the stationary distributions found analytically with those found by numerical simulations and find good agreement. Indeed, the Markov chain analysis can be used to check under what conditions a limiting distribution exists, so that numerical simulations will converge, and how long they need to be run to yield accurate results.

**6.1 Uniform IEI Distribution.** Consider system 6.1 with constant inhibition, which may be on or off. We take the IEIs to be distributed uniformly on [30,70] msec, except for the first such interval after each reset, which is chosen from a uniform distribution on [20,60] msec (see remark 7 below). Using the bin definitions 3.1 and 3.2, with this minor adjustment to  $I_1$ , we have  $I_1 = [w_{RK}^E \cdot 20, w_{RK}^E \cdot 50)$ ,  $I_2 = [w_{RK}^E \cdot 50, w_{RK}^E \cdot 80)$ ,  $\dots$ ,  $I_{N-1} = [w_{RK}^E \cdot 20 + (N - 2)30, w_{LK}^E]$ ,  $I_N = (w_{LK}^E, w_{FP}^0)$ . For the default parameters of system 6.1, inhibition held at  $s_{inh} = 0$ , and the excitation characteristics described, simulation of the TC model, equation 6.1, for one passage through the silent phase shows that  $N = 3$ , while with inhibition at  $s_{inh} = 1$ , we find  $N = 5$ .

With  $s_{inh} = 0$ , the states of the Markov chain are (1, 1), (2, 1), (2, 2), (3, 2), (3, 3), with bin boundaries defined from the one-time simulation. The transition matrix for this case, call it  $P^0$ , is computed analytically in appendix A and appears in equation A.1. The unit-dominant eigenvector of  $(P^0)^T$  gives the limiting distribution,

$$v^0 = [.3404 \ .1135 \ .0922 \ .3617 \ .0922]^T. \quad (6.2)$$

As discussed in section 4, the values of  $v^0$  represent the likelihood that a cell is found in a given state, if state membership is recorded just prior to the onset of an excitatory input. For comparison, we simulated a single cell, modeled by equation 6.1, with the technical modification mentioned in remark 8 below, over 70 sec, after an initial transient of 10 sec. This

simulation yielded the vector

$$v_{num}^0 = [0.3276 \ 0.1289 \ 0.0878 \ 0.3629 \ 0.0878]^T$$

of proportions of inputs during which the cell belonged to each relevant state, which agree nicely with the analytically computed expectations  $v^0$  in equation 6.2. Over the entire simulation, the cell never failed to fire to three consecutive inputs.

Grouping our analytical values by bins indicates that just before onset of excitation, on 34.04% of the observations, we expect  $w \in [w_{RK} \cdot 20, w_{RK} \cdot 50)$ , on 20.57% of the observations, we expect  $w \in [w_{RK} \cdot 50, w_{RK} \cdot 75.5)$ , and on 45.39% of the observations, we expect  $w > w_{RK} \cdot 75.5$ . In particular, this implies that a cell will fire to roughly 45% of its inputs for these choices of parameters. Further, from equations 4.3 and 4.4 with  $Q$  values given by entries of  $v^0$ , it is expected that a successful input will be followed by 1.20 inputs that fail to elicit a spike, before the next successful input occurs; this is in good agreement with direct simulation results showing a mean of 1.19 unsuccessful inputs between successful ones. As discussed in section 5, these results can also be interpreted in terms of a population of identical cells as long as the cells receive independent realizations of the input.

With nonzero constant inhibition, given by  $s_{inh} = 1$ , the states of the Markov chain are (1,1), (2,1), (2,2), (3,2), (3,3), (4,2), (4,3), (4,4), (5,2), (5,3), (5,4), and (5,5). The transition matrix,  $P^I$ , is computed analytically in appendix B and appears in equation B.1. In this case,  $(P^I)^T$  has the unit-dominant eigenvector  $v^I$ , which is shown below together with the distribution of states listed in vector  $v_{num}^I$ . The latter are obtained from direct numerical simulation for 80 sec, with a transient consisting of the first 10 sec removed from consideration:

$$v^I = [0.2290 \ 0.0763 \ 0.0859 \ 0.1622 \ 0.0215 \ 0.0569 \ 0.0624 \ 0.0005 \ 0.0004 \\ 0.2211 \ 0.0833 \ 0.0005]^T$$

$$v_{num}^I = [0.2272 \ 0.0784 \ 0.0726 \ 0.1927 \ 0.0194 \ 0.0388 \ 0.0669 \ 0.0022 \ 0.0007 \\ 0.2171 \ 0.0820 \ 0.0002]^T.$$

Grouping the states ( $I_5, j$ ) reveals that a cell will fire in response to about 30% of its inputs. This failure rate is higher than in the case of  $s_{inh} = 0$ , which is to be expected because inhibition changes the locations of  $w_{LK}^E$  and  $w_{RK}^E$ , so that the time to evolve from  $w_{RK}^E$  to  $w_{LK}^E$  is longer with inhibition on than with inhibition off. Similarly, based on  $v^I$ , the case of  $s_{inh} = 1$  has a substantially higher expected number of failed inputs between spike-inducing inputs, namely,  $E_f = 1(0.0013) + 2(0.7240) + 3(0.2731) + 4(0.0016) = 2.28$  from equations 4.3 and 4.4, compared to the 1.20 expected in the case of  $s_{inh} = 0$ . Direct numerical simulation gives a similar estimate of  $E_f = 2.35$  in this case.

**Remark 7.** In the above calculation, each time interval from the offset of one input to the onset of the next was chosen from a uniform distribution on  $[20,60]$  msec. Suppose that we were to fix the total duration of each excitatory input at 10 msec. Since  $\varepsilon \neq 0$  in simulations, even with this constant input duration, the part of the input duration remaining after the cell is reset from the active phase would vary after different spiking events. This variation can be handled easily, as discussed in remark 4, and results in a distribution of IEIs  $T$  with support on  $[20+x,70]$  msec, where  $x$  is the minimal duration of input remaining after reset. However, to maintain a uniform IEI distribution, we chose to adjust the simulations by simply turning off the input each time a firing cell is reset or, equivalently, setting the input duration equal to 0 on the slow timescale. As a result, the distribution for the first IEI after reset was supported on  $[20,60]$  msec rather than on  $[30,70]$  msec.

**Remark 8.** For consistency with section 3, we modified model 6.1 to make the cell oscillatory in the presence of excitation. To do this, we simplified the dynamics to the form  $w' = (w_\infty - w)/\tau_w$  whenever  $v < -55$ , for constants  $w_\infty = .61$  and  $\tau_w = 407$ , which were chosen to give nice bin boundary values. We also made a related technical adjustment to simplify the presentation of these example results, related to the nonzero duration of excitation. If an excitatory input arrives but fails to make a cell fire, then the cell jumps from the left branch of  $\mathcal{N}^0$  to the left branch of  $\mathcal{N}^E$ , and it evolves on this branch of  $\mathcal{N}^E$  while the input is on. The rates of flow on the left branches of  $\mathcal{N}^0$  and  $\mathcal{N}^E$  may differ, however. Thus, the time a cell takes to travel from one value of  $w$  to another in the silent phase may depend on how many inputs the cell receives during the passage. This can easily be taken into account in the above calculations by making appropriate adjustments to bin boundaries, but this would clutter the exposition. Hence, we instead adjusted the flow in our simulations of equation 6.1 in this example so that the  $w$  dynamics was identical on the left branches of  $\mathcal{N}^0$  and  $\mathcal{N}^E$ . In theory, the way that we did this introduces the possibility that solutions may escape from the left branch of  $\mathcal{N}^0$  in the vicinity of  $w_{LK}^0$  and fire without receiving input, since  $w_{LK}^0 < w_\infty$ . However, in practice, this does not occur because  $w_{LK}^0$  is sufficiently large, relative to the IEIs, that it is never reached.

**6.2 Normal, or Other, IEI Distributions.** If IEIs are taken from a nonuniform distribution, we can still use equation 3.5 to obtain the transition matrix elements analytically, albeit with numerical evaluation of the integrals that arise. These integrals are analogous to those given in appendixes A and B for the uniform case. Once the transition matrix is obtained, the limiting distribution for the Markov chain is computed as the unit-dominant eigenvector of its transpose, as previously.

For example, consider IEIs of the form  $T = t_{ref} + X$ , where  $t_{ref}$  is a fixed constant and  $X$  is selected from a truncated normal distribution. In

particular, suppose that  $t_{ref} = 20$  msec, that  $\tilde{X}$  is selected from a normal distribution with mean 20 msec and standard deviation 10 msec, and that

$$X = \begin{cases} 0, & \tilde{X} < 0, \\ \tilde{X}/M_X, & 0 \leq \tilde{X} \leq 40, \\ 40, & 40 < \tilde{X}, \end{cases} \quad (6.3)$$

where  $M_X$  is a constant correction factor such that  $\int_{\mathbf{R}} X = 1$ . This is a reasonable choice that keeps IEs within the bounds present in the example in the previous section. For this example, with other simulation parameters fixed as in the previous section, including  $s_{inh} = 0$  and an input duration of 10 msec, and the same adjustment mentioned in remark 8, we obtained the transition matrix  $(P_n^0)$  given in equation A.2, corresponding to states (1, 1), (2, 1), (2, 2), (3, 2), (3, 3). The dominant eigenvector  $v_n^0$  of  $(P_n^0)^T$  matches closely with a vector  $(v_n^0)_{num}$  obtained from direct counting of state membership in the last 90 sec of a 100 sec numerical simulation:

$$\begin{aligned} v_n^0 &= [.4073 \ .0670 \ .0594 \ .4108 \ .0594]^T \\ (v_n^0)_{num} &= [.3883 \ .0812 \ .0625 \ .4070 \ .0610]^T. \end{aligned}$$

Here, the subscript  $n$  simply indicates the use of a normal distribution of IEs. Based on these results, we expect that a cell will respond to approximately 47% of the inputs, with an average of 1.15 failures between successful spikes from equations 4.3 and 4.4. This agrees nicely with the estimate 1.13 that we obtained from direct numerical simulations.

For completeness, we conclude with the results of an analogous calculation done with  $s_{inh} = 1$ . This yields the transition matrix  $P_n^1$  given in equation B.2, corresponding to states (1, 1), (2, 1), (2, 2), (3, 2), (3, 3), (4, 2), (4, 3), (5, 2), (5, 3), (5, 4). The corresponding dominant eigenvector  $v_n^1$ , and an example vector  $(v_n^1)_{num}$  of state occupancy probabilities from direct simulations, are

$$\begin{aligned} v_n^1 &= [.2638 \ .0438 \ .0672 \ .2234 \ .0072 \ .0169 \ .0701 \ .2133 \ .0942]^T \\ (v_n^1)_{num} &= [.2587 \ .0505 \ .0697 \ .2132 \ .0121 \ .0263 \ .0637 \ .2329 \ .0728]^T, \end{aligned}$$

where we have omitted the (5,2) entry since the probability of occupancy there is less than  $0.5 \times 10^{-5}$ . These results imply that a cell with  $s_{inh} = 1$  will respond to approximately 31% of excitatory inputs and is thus less reliable than a cell with  $s_{inh} = 0$ . The average number of failures between spikes is 2.27, from equations 4.3 and 4.4, which is similar to the 2.24 obtained from direct simulations and exceeds that found with  $s_{inh} = 0$ .

## 7 Inhibitory and Excitatory Inputs

---

We next consider the more complex case in which the postsynaptic cell receives a stochastic excitatory input train while subjected to modulation by an inhibitory input. The corresponding analysis illustrates how switches between any pair of epochs with different state transition characteristics can be handled naturally within the Markov chain framework through products of transformation matrices. In particular, the same type of analysis could be done if both input trains were excitatory, with different statistics. Moreover, in the next section of the letter, the example that we present will be discussed in connection with a possible mechanism for the therapeutic effectiveness of DBS.

**7.1 Transition Matrices.** In this section, we assume that for a system of the form 2.1 with input given by equation 2.2, the function  $s_{inh}(t)$  turns on and off abruptly, with a relatively long period between transitions. In the previous section, we discussed how to derive the transition matrices  $P^I$  and  $P^0$  for the case of constant inhibition of any level. Our next goal is to derive transition matrices  $P^{0 \rightarrow I}$  and  $P^{I \rightarrow 0}$ , encoding the probabilities of passing between various states during the onset and offset of inhibition, respectively. Using these matrices, we can form a transition matrix for the time from one inhibitory offset (or onset) to the next, by matrix multiplication.

One complication in this derivation is that the bin boundaries differ between the cases of zero and nonzero inhibition. Even with the assumption that the rate of evolution in the silent phase is independent of input level, differences in bin boundaries remain due to differences in right knee positions, leading to different starting points in the silent phase. Similarly, differences in left knee positions lead to different cutoffs for firing. To make this explicit, in the following analysis, let  $\{S_j^0\}_{j=1}^{N_0}$  denote the ordered states for the Markov chain formed when inhibition is off, which we call the inhibition-off Markov chain, and let  $\{S_j^I\}_{j=1}^{N_I}$  denote the states for the Markov chain defined when inhibition is on, which we call the inhibition-on Markov chain. We use the notation  $(I_k^0, l)$  or  $(I_k^I, l)$  for the states in these collections.

A second difficulty is that due to the stochasticity of the input trains, a change in inhibition level may occur at any time relative to the start of the particular IEI during which it happens, or even at a time when excitation is on. An example of how the resulting bin membership depends on the inhibition onset time is illustrated schematically in Figure 6.

To handle both of these issues, we define the transition matrix  $P^{0 \rightarrow I}$  for the onset of inhibition in the following way. First, note that there will be a final iteration of the inhibition-off Markov chain, before inhibition arrives, after which the cell will lie in a state  $S_u^0$  for some  $u$ . During the next IEI, inhibition arrives. At the end of this IEI, the cell will lie in a state  $S_v^I$  for some  $v$ . For  $i = 1, \dots, N_0$  and  $j = 1, \dots, N_I$ , let the  $(i, j)$  entry of  $P^{0 \rightarrow I}$  denote the

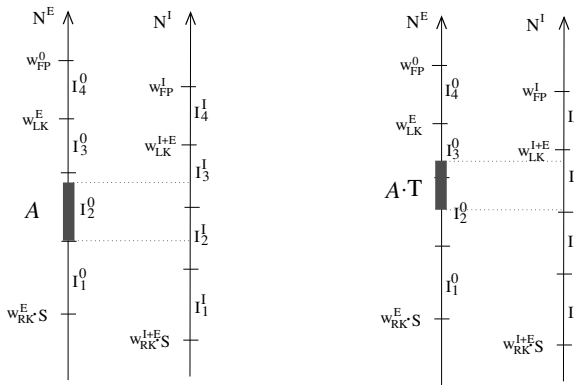


Figure 6: A schematic depiction of the two difficulties encountered when defining the matrix  $P^{0 \rightarrow I}$ . (Left) An ensemble of cells  $A$  in state  $(I_2^0, l)$  is mapped to two bins,  $I_2^I$  and  $I_3^I$ , when inhibition turns on. (Right) The same ensemble gets mapped only to the bin  $I_3^I$  if inhibition turns on a time  $T$  later than in the left panel.

probability that  $u = i$  and  $v = j$ . Recall that the states of the inhibition-off Markov chain, by definition, take the form  $(I_k^0, l)$ , where  $l$  gives a count of IEIs since last reset; thus, many elements of  $P^{0 \rightarrow I}$  will be zero.

There are several important advantages to basing the cycle length on only excitatory input times rather than the time when inhibition turns on. This definition of  $P^{0 \rightarrow I}$  renders irrelevant the bins into which an ensemble is mapped by the onset of inhibition itself (e.g., Figure 6), since bin membership is not checked when inhibition is turned on but is instead checked at the end of the IEI during which the inhibitory onset occurs. Moreover, in this formulation, it does not matter whether inhibition turns on while the excitation is still on or after it is off, if we continue to assume that the rate of silent phase evolution is input independent (assumed in remark 8). Whether the last excitatory input that arrives before the onset of inhibition causes the cell to fire, or fails to do so, is determined by the knee positions without inhibition, and if a firing occurs, instantaneous reset to  $w_{RK}^E$  follows. We neglect the probability zero case of excitation and inhibition turning on at precisely the same moment, and therefore if a cell fires, then inhibition will always turn on after the cell is reset.

As previously, let  $w_{LK}^{I+E}$ ,  $w_{RK}^{I+E}$  denote the knees of the nullcline  $\mathcal{N}^{I+E}$ , corresponding to the case when both excitation and inhibition are on. One additional complication may arise due to the fact that  $w_{RK}^E < w_{RK}^{I+E}$ . That is, at the onset of inhibition,  $w$  may lie below the lower boundary of the inhibition-on partition. To account for this possibility requires the inclusion of additional bins in this partition, with a corresponding adjustment of the matrix  $P^I$  to allow for matrix multiplication.

We define the transition matrix  $P^{I \rightarrow 0}$ , for the offset of inhibition, analogously to the case of  $P^{0 \rightarrow I}$ . That is, there will be a final iteration of the inhibition-on Markov chain, before inhibition turns off, after which the cell will lie in a state  $S_u^I$ . During the next IEL, inhibition turns off. At the end of this IEL, the cell will lie in a state  $S_v^0$ . The  $(i, j)$  entry of  $P^{I \rightarrow 0}$  denotes the probability that  $u = i$  and  $v = j$ . The complication in this case is that postinhibitory rebound (PIR) may occur if, when the offset of inhibition occurs, either excitation is off and  $w > w_{LK}^0$  or excitation is still on and  $w > w_{LK}^E$ . Rebound leads to reinjection into the silent phase followed by evolution there. However, the duration of this evolution, from the time of reinjection to the time that the next excitatory input arrives, depends on when the inhibition turned off, relative to the time of the previous input, which complicates calculations.

Assuming that  $P^{0 \rightarrow I}$ ,  $P^{I \rightarrow 0}$  can be computed, the appropriate transition matrix for the case of excitatory and inhibitory input trains is obtained by multiplication of the transposes of the separately computed transition matrices  $P^0$ ,  $P^I$ ,  $P^{0 \rightarrow I}$ , and  $P^{I \rightarrow 0}$ . Specifically, let  $[M]^T$  denote the transpose of matrix  $M$ , and let  $(M)^n$  denote  $M$  to the  $n$ th power. Suppose that  $n$  IELs occur in the absence of inhibition, that inhibition arrives during the next IEL, that  $m$  additional IELs occur with inhibition on, and that inhibition turns off again on the next IEL. In this case, the  $(j, i)$  entry of the matrix

$$[P^{I \rightarrow 0}]^T ([P^I]^T)^m [P^{0 \rightarrow I}]^T ([P^0]^T)^n$$

gives the probability that a cell that starts in state  $S_i^0$  of the inhibition-off partition ends up in state  $S_j^0$  after the sequence of  $n + m + 2$  IELs described above. Of course, when the IELs and the durations of inhibitory on and off periods are selected randomly from distributions, the probabilities that different numbers  $(m, n)$  of excitatory inputs arrive during these periods are also random; in appendix C, these are calculated for the example of uniform distributions.

In the general discussion given here, let us assume that  $m, n \geq 0$  are bounded above by  $M, N < \infty$ , respectively. Suppose that over a long time period, we check the cell's state membership at the first onset of excitation following each inhibitory offset. We would like to claim that in the asymptotic limit, the proportion of these trials for which a cell will belong to each inhibition-off state is given by the entries of the unit-dominant eigenvector of the matrix

$$\sum_{m=0}^M \sum_{n=0}^N c_{m,n} [P^{I \rightarrow 0}]^T ([P^I]^T)^m [P^{0 \rightarrow I}]^T ([P^0]^T)^n, \tag{7.1}$$

where each coefficient  $c_{m,n}$  denotes the probability of occurrence of the corresponding exponent pair  $(m, n)$ , some of which may be 0. Substantiating

this claim necessitates justifying whether this eigenvector exists and truly represents a limiting distribution. This will be true if the matrix in equation 7.1 is irreducible and aperiodic, as discussed in section 4. Recall that the proof of theorem 2 gives an upper bound  $b$  for the number of inputs after which occupancy of all states is guaranteed, under the assumptions of the theorem, for constant inhibition. Now, let  $b_I, b_0$  denote the respective upper bounds for matrices  $P^I, P^0$ , based on the IEI distribution. A sufficient pair of conditions to guarantee the existence of a limiting distribution for equation 7.1 is that if the probability  $p(m) > 0$ , then  $m \geq b_I$ , while if  $p(n) > 0$ , then  $n \geq b_0$ . If these conditions are violated, the states of the system may still tend to some limiting distribution, particularly if  $p(m), p(n)$  are substantial for some values above the respective bounds, but this must be verified numerically.

Similarly, the unit-dominant eigenvector of the matrix,

$$\sum_{m=1}^M \sum_{n=1}^N c_{m,n} [P^{0 \rightarrow I}]^T ([P^0]^T)^n [P^{I \rightarrow 0}]^T ([P^I]^T)^m, \tag{7.2}$$

if it exists and represents a limiting distribution, gives the expected proportions of trials for which a cell will belong to each inhibition-on state  $(I_k^I, l)$  at the moment of arrival of the first excitatory input after inhibition turns on. The dominant eigenvectors of the matrices

$$\begin{aligned} &\sum_{m=1}^M \sum_{n=1}^N c_{m,n} ([P^0]^T)^n [P^{I \rightarrow 0}]^T ([P^I]^T)^m [P^{0 \rightarrow I}]^T \\ &\sum_{m=1}^M \sum_{n=1}^N c_{m,n} ([P^I]^T)^m [P^{0 \rightarrow I}]^T ([P^0]^T)^n [P^{I \rightarrow 0}]^T \end{aligned}$$

have similar interpretations.

**Remark 9.** In fact, justifying the existence of the limiting distribution for the matrix in equation 7.2 requires an additional technical adjustment, relative to that for matrix 7.1. The added complication arises because the fixed point of  $\mathcal{N}^I$  is higher than that of  $\mathcal{N}^0$ , which may lead to a violation of irreducibility. This is simply a technical point and can be handled by replacing  $([P^I]^T)^m$  by the product of a sequence of nonidentical matrices that incorporate successively larger numbers of states, assuming  $m$  is not too small.

**7.2 TC Cell Example Revisited: Uniform Distributions.** Consider again the TC model equation 6.1. We focused on inhibitory onset and computed the transition matrices from equation 7.2 analytically, using

equation 3.5 as in the constant inhibition cases discussed in appendixes A and B, under the assumptions that the intervals from excitatory offsets to onsets are selected from a uniform distribution on [20,60] msec, that the excitatory duration is fixed at 10 msec, and that the durations of both the inhibitory inputs and the time intervals between inhibitory inputs are selected from a uniform distribution on [125,175] msec. In this example, the coefficients  $c_{m,n} = p(m)p(n)$  in equation 7.2 can also be computed analytically, and we discuss some details of this calculation in appendix C. After the  $p(m)$  are computed, the dominant eigenvector  $v^{0 \rightarrow I}$  of matrix 7.2 can be obtained. We compare  $v^{0 \rightarrow I}$  to its counterpart,  $v_{num}^{0 \rightarrow I}$ , generated numerically from 301 inhibitory onsets during the last 90 sec of a 100 sec simulation:

$$v^{0 \rightarrow I} = [.3530 \ .0801 \ .1598 \ .2558 \ .0333 \ .0677 \ .0363 \ 0 \ 0 \ .0140 \ 0 \ 0]^T$$

$$v_{num}^{0 \rightarrow I} = [.3089 \ .1030 \ .0897 \ .2724 \ .0199 \ .0432 \ .0698 \ 0 \ 0 \ .0664 \ .0066 \ 0]^T.$$

The states here are exactly those listed in section 6 for the uniform IEI distribution with  $s_{inh} = 1$ : (1,1), (2,1), (2,2), (3,2), (3,3), (4,2), (4,3), (4,4), (5,2), (5,3), (5,4), and (5,5). Note that the zero entries here signify values less than  $0.5 \times 10^{-5}$ . These states are included in the chain because they are reached after inhibition stays on sufficiently long, since inhibition shifts the  $v$ -nullcline to higher  $w$ -values. However, the probability of membership in these states just after inhibition turns on is negligible.

The agreement between  $v^{0 \rightarrow I}$  and  $v_{num}^{0 \rightarrow I}$  is fairly good, although not as good as in the case of constant inhibition in section 6. This is presumably due to errors introduced by some minor simplifying assumptions that we made, which are discussed in remark 10. The distribution  $v^{0 \rightarrow I}$  indicates that a cell will be expected to fire well under 10% of the time to the first input that arrives just after the onset of inhibition. This low number fits the prediction of phase plane and bifurcation analysis, which implies that the onset of inhibition interferes with responsiveness to the subsequent excitatory input (Rubin & Terman, 2004). Moreover, the full distribution  $v^{0 \rightarrow I}$  characterizes the expected behavior of the cell after this first excitatory input. In particular, note that the cell will be in the (1,1) state, corresponding to the lowest slow variable values, on the arrival of over 30% of such inputs, which is a significant increase over the likelihood of membership in this state in the  $s_{inh} = 1$  case. Hence, the compromise of responsiveness by rhythmic inhibition will endure beyond the first excitation after inhibitory onset.

**Remark 10.** Recall that PIR, or rebound, refers to the firing of a spike immediately on the removal of inhibition. Although we focus on equation 7.2, and hence on the limiting distribution  $v^{0 \rightarrow I}$  corresponding to the onset of inhibition, in the above example, we still must consider PIR in the calculation of the elements of the matrix  $P^{I \rightarrow 0}$ , which appears in equation 7.2. Since the possibility of rebounding in general, and in particular rebounding

and reaching  $I_2$  before the arrival of the next excitation, is relatively small for our parameter values, we make the simplifying assumption that after PIR, a cell can reach only  $I_1$  before the next excitation arrives. To maintain tractability, we also neglect the fact that  $w_{RK}^{I+E} > w_{RK}^E$ , based on the fact that the right knees are fairly close for  $g_{inh} = 0.12$ . These approximations do introduce some error into our results.

**7.3 TC Cell Example Revisited: Normal Distributions.** For comparison to direct numerical simulation, we also calculated the transition matrices and dominant eigenvector when IEs were selected from the truncated normal distribution described earlier (see equation 6.3), with inhibition on and off durations selected from a similar truncated normal distribution. The distribution for on and off intervals of inhibition was supported on [125,175] msec and had mean 150 msec, as in the uniform distribution example. To compute the relevant dominant eigenvector, as done above in the uniform distribution case, we need coefficients  $c_{m,n}$ , which we computed as  $c_{m,n} = p(m)p(n)$  from the numerically obtained probabilities  $p(1) = .0014$ ,  $p(2) = .1625$ ,  $p(3) = .6763$ ,  $p(4) = .1625$ ,  $p(5) = .0014$ , with  $p(j) = 0$  for  $j \geq 6$ . In this case, we used transition probabilities obtained from long-time simulations to compute the transition matrices  $P_n^{I \rightarrow 0}$ ,  $P_n^{0 \rightarrow I}$ , which we do not display here, although these could have been computed from equation 3.5 as well. The dominant eigenvector  $v_n^{0 \rightarrow I}$ , corresponding to state occupancy at the arrival time of the first excitatory input after inhibitory onset, and an example of the distribution of states  $(v_n^{0 \rightarrow I})_{num}$  obtained from the last 90 sec of a 100 sec simulation are

$$v_n^{0 \rightarrow I} = [.3354 \ .0463 \ .1233 \ .3685 \ .0083 \ .0394 \ .0350 \ .0439 \ 0 \ ]^T$$

$$(v_n^{0 \rightarrow I})_{num} = [.3984 \ .0549 \ .1071 \ .3132 \ .0082 \ .0302 \ .0384 \ .0467 \ .0027 \ ]^T,$$

for states (1, 1), (2, 1), (2, 2), (3, 2), (3, 3), (4, 2), (4, 3), (5, 3), (5, 4), with the subscript  $n$  for normal as previously. These results show that a cell can be expected to fire reliably to the first excitatory input after the onset of inhibition less than 5% of the time, and it will lie in the (1,1) state on the arrival of over 30% of such inputs, as also seen in the uniform distribution example.

## 8 Explicit Connection to Parkinsonian Reliability Failure \_\_\_\_\_

In PD, the inhibitory output from the basal ganglia may become rhythmic. DBS eliminates this rhythmicity, leading to inhibition from the basal ganglia that is elevated but, when summed over all inputs to a cell, is roughly constant, possibly with fast oscillations around a high constant level. A possible mechanism for the induction of motor symptoms in PD and for their amelioration by DBS, analyzed in Rubin and Terman (2004), is that

rhythmic basal ganglia inhibitory outputs periodically compromise TC response reliability, while the regularization of these outputs by DBS restores responsiveness. The drastic drop in the number of TC cells expected to fire and the accumulation of cells in states far from firing threshold found just after inhibitory onset in the case of rhythmic inhibition in our examples, relative even to the case of elevated but constant inhibition, offers a strong demonstration of the feasibility of this idea. The approach that we have taken to obtain these results is based on limiting distributions, and hence eliminates the possibility of spurious outcomes due to transient effects in simulations.

Suppose that we adjust parameters to an extreme case, so that TC cells fire in response to every excitatory input when  $s_{inh} = 0$  and when  $s_{inh} = 1$ . In terms of the slow variable, these conditions become

$$w_{RK}^E \cdot S > w_{LK}^E \quad (8.1)$$

and

$$w_{RK}^{I+E} \cdot S > w_{LK}^{I+E}.$$

Even with these strong conditions, we still find some failures when inhibition turns on and off rhythmically. In this case, we can read off from  $v^{0 \rightarrow I}$  the probabilities with which a cell will experience each possible number of failures due to inhibitory onset, as seen in the examples discussed above. In particular, even if no failures occur when inhibition is held at a constant level, there may be multiple failures following inhibitory onset if the difference  $w_{RK}^{I+E} - w_{RK}^E$  is large.

Inhibitory offset may lead to response failure as well, through PIR. Cells that rebound when inhibition turns off are reset to  $w_{RK}^E$ . The assumption of reliability in the inhibition-off case implies that inequality 8.1 holds. However, the time from the offset of inhibition until the arrival of the next excitatory input may be less than  $S$ , since inhibition may turn off at any moment in the IEL. Therefore, the time  $t^*$  from PIR to the next arrival of excitatory input may be less than  $S$ , and a response failure can follow PIR. Finally, after such a failure, relay will proceed reliably under assumption 8.1, since a cell will lie at  $w_{RK}^E \cdot t^* > w_{RK}^E$  after its first failure. In summary, even under the assumption of perfect TC relay reliability in the constant inhibition case, multiple relay failures can occur following inhibitory onsets, while inhibitory offsets can induce PIR, possibly followed by a single relay failure.

## 9 Discussion

---

We have considered a fast-slow excitable system subject to a stochastic excitatory input train, and we have shown how to derive an irreducible

Markov chain that can be used analytically to compute the system's firing probability to each input, expected number of response failures between firings, and distribution of slow variable values between firings, in the infinite-time limit. We have illustrated this analysis on a model TC cell subject to a uniform or a truncated normal distribution of excitatory synaptic inputs, in the cases of constant inhibition and of inhibition that switches abruptly between two levels. The analysis generalizes to any pair of input trains, excitatory or inhibitory and synaptic or not, that switch, with distinct frequencies, between discrete on and off states. In such cases, an appropriate transition matrix, analogous to equation 7.1, can always be derived. This approach also can be extended to other models, such as the Haken (2002) or Kuramoto (1984) models, featuring a single variable that builds up to a threshold, mediates an instantaneous spike, and experiences a reset, possibly followed by a refractory period. In this vein, we expect that extension to integrate-and-fire type models should be possible, but the details of handling nonmonotone changes in voltage would need to be worked out.

In the TC cell case, our results generalize earlier findings suggesting how the modulation of inhibitory outputs of the basal ganglia can compromise TC responsiveness to excitatory inputs, with possible relevance to PD and DBS (Rubin & Terman, 2004). The method used here goes beyond the direct counting of failed responses to a sequence of inputs that was done previously, by deriving information about the complete limiting distribution of states in the TC cell Markov chain. More generally, basal ganglia output areas in rat show abrupt firing rate fluctuations on the timescale of seconds-to-minutes even in non-parkinsonian states (Ruskin et al., 1999), and the ideas we introduced could be used to consider how different fluctuation characteristics affect TC reliability. TC cells are also inhibited by thalamic reticular (RE) cells, which are targets of excitatory corticothalamic inputs. Cortical oscillations, particularly abrupt transitions between cortical up and down states (Steriade, Nunez, & Amzica, 1993a; Cowan & Wilson, 1994), could naturally lead to jumps in the levels of inhibition from RE cells to TC cells, providing an alternative source for the type of inhibition that we consider. In this context, our results provide a way to quantify the expected extent of the transient loss of thalamic relay reliability during the transitions between up and down states of different depths, as well as the likelihood that transitions from down to up will be signaled by PIR thalamic bursts (Steriade, Nunez, & Amzica, 1993b). Huertas et al. (2005) have also considered the relay properties of TC cells, specifically those in the dorsal lateral geniculate nucleus, in the presence of RE inhibition, using simulations of an integrate-and-fire-or-burst model with an oscillatory driving input based on retinal ganglion cell activity. In their simulations, as found here and in previous work such as Rubin and Terman (2004), rhythmic inhibition to TC cells led to TC bursts and a failure of TC cells to respond to excitatory signals, although TC-RE interactions in their model gave rhythmic TC bursting

phase-locked to the driving stimulus, which would not be present for the types of synaptic drive we consider.

We have proved that under general conditions, the Markov chain we derived is irreducible and aperiodic and hence has a limiting distribution, which can be computed analytically using equation 3.5, using a one-time simulation for establishment of bin boundaries. This finding contrasts with Monte Carlo simulations, in which convergence properties cannot be forecast and transient effects may be a concern. Our analysis also explains why a limiting distribution will not exist when these conditions break down, and hence these results, even without the full calculations, can be used to decide whether Monte Carlo simulations are a reasonable option. It is interesting to consider the minimal requirements for the application of our Markov chain ideas. Application of this approach will be possible whenever a driven system can be characterized as having a single (or single dominant) slow recovery process or other variable that builds up to a firing threshold in the silent phase, the transition probabilities between states in the silent phase can be estimated from the behavior of this variable, and the statistics of the input to the cell are known. Consideration of the minimal requirements for the experimental characterization of such transition probabilities for a neuron, possibly along the lines of phase response curve estimation, remains an interesting avenue for future consideration.

Our work is related to two earlier studies in which a Markov operator was derived to track transitions between oscillator phases, relative to sinusoidal forcing, at successive jump-up (Doi et al., 1998) or threshold-crossing (Tateno & Jimbo, 2000) times, in the presence of noise. Neither of these works, however, used a Markov chain to track transitions linked to successive input arrivals but not to firing events. Moreover, neither arrived at analytically computable transition probabilities or proved the existence of a limiting distribution, as we have done. A nice feature of the previous letters was the numerical tracking of subdominant eigenvalues to identify bifurcations, defined in a stochastic sense, relating to changes in mode locking. The approach that we have presented could also be used to study bifurcations. For example, as mentioned in remark 6, a change in the range of IEs can cause the transition probability between a pair of states to switch from zero to nonzero, which may abruptly change the existence, or the nature, of the corresponding limiting distribution.

As a related alternative approach, one could try to analyze the long-term behavior of a cell by studying the random dynamical system  $w_{n+1} = M_T(w_n)$ , where the interinput interval  $T$  is a random variable with a known density (Lasota & Mackey, 1994). If it could be found, then the limiting density for the variable  $w$  could be used to compute the statistics of interest for the cell. However, finding this limiting density is in general quite difficult. The Markov chain approach that we have presented can in fact be viewed as a discretization of this procedure. As a result, we recover a coarsely grained

version of the full limiting density for  $w$ , which is sufficient to determine the statistics of interest.

In a series of letters (Othmer & Watanabe, 1994; Xie et al., 1996; Othmer & Xie, 1999), Othmer and collaborators studied the application of step function forcing to a piecewise linear excitable system similar to those that we consider. In their work, which focused on the existence of mode-locked (harmonic or subharmonic) solutions and on chaos, they used a map and defined states as we do, but their states were based on positions of the knees of nullclines and their projections to other nullclines rather than the flow along branches of nullclines, and they did not consider a Markov chain for transitions between states. Moreover, their analysis was restricted to periodic forcing, whereas ours accommodates, and indeed is particularly well suited for, stochasticity in input timing. LoFaro and Kopell (1999) also used 1D maps to study a forced excitable system, but in their work, the excitable system was a neuron mutually coupled via inhibitory synapses to an oscillatory cell and the map was a singular Poincaré map, with each iteration corresponding to the time between jumps to the active phase. Similarly, Keener, Hoppensteadt, and Rinzel (1981) and subsequent authors have used firing time maps to study mode locking in integrate-and-fire and related models with periodic stimuli. Alternatively, other works have used 1D maps based on interinput intervals to study mode-locked, quasi-periodic, and chaotic responses of excitable systems to periodic, purely excitatory inputs (Coombes & Osbaldestin, 2000; Ichinose et al., 1998).

Clearly, the transformation of some combination of excitatory and inhibitory synaptic inputs into postsynaptic neuronal responses is a fundamental operation present within any nontrivial nervous system. As a result, various manifestations of this transformation have been studied, computationally and experimentally, by many researchers. In our work, as in Smith and Sherman (2002), we consider the excitatory input stream as a drive to the postsynaptic cell and the inhibitory input as a modulation that alters the cell's responsiveness to its drive. We neglect such intriguing effects as long-term synaptic scaling (Desai, Cudmore, Nelson, & Turrigiano, 2002), changes in intrinsic excitability (Aizenman, Akerman, Jensen, & Cline, 2003), and changes in the balance of excitation and inhibition (Somers et al., 1998), which could become relevant in the asymptotic limit, as well as the effect of attention (Tiesinga, 2005). Moreover, we assume that successful thalamic relay consists of single-spike responses to an input train, neglecting the idea that by virtue of their stereotyped form and reliability, thalamic bursts may serve a relay function (Person & Perkel, 2005; Babadi, 2005). Other authors have considered how variations in intrinsic properties of postsynaptic cells determine the input characteristics that induce these cells to spike most reliably (Fellous et al., 2001; Schreiber, Fellous, Tiesinga, & Sejnowski, 2004) and how neuronal processing varies under more general changes in input spike patterns than the ones that

we have considered here (e.g., Hunter & Milton, 2003; Tiesinga & Troups, 2005). While these issues are beyond the scope of this work, our approach can accommodate input trains that vary stochastically in a variety of ways (e.g., see remarks 3 and 4), and hence it may be well suited for the future exploration of such issues.

## Appendix A: TC Cell with $s_{inh} = 0$

---

With  $s_{inh} = 0$ , a cell that has just spiked is guaranteed to spike again after at most  $N = 3$  subsequent inputs. Although the intervals  $I_k$  are defined in terms of intervals of the slow variable  $w$ , clearly there is also a particular time interval associated with each  $I_k$  (see remark 11 below). In the particular model, equation 6.1, with  $s_{inh} = 0$ , these time intervals are  $[20, 50)$ ,  $[50, 75.5)$ ,  $[75.5, \infty)$ , where  $w_{RK}^E \cdot 75.5 \approx w_{LK}^E$ . In practice, we used a simulation protocol, rather than determination of the left knee of  $\mathcal{N}^E$  directly from equation 6.1, to compute the value 75.5. That is, we found 75.5 to be the minimum value of  $t$  such that, given an initial condition with  $w = w_{RK}^E \cdot t$  and with  $v$  at the corresponding position on the left branch of  $\mathcal{N}^0$ , the model cell would fire in response to an excitatory input of duration 10 msec. This adjustment represents the modification to  $w_{LK}^E$  discussed in remark 4 and is therefore consistent with the rest of the analysis that we present.

Using these time intervals allows us to compute the transition probabilities between states  $(I_k, j)$  for  $j, k = 1, \dots, 3$ , with  $j \leq k$ . Let  $p_{(k_1, j_1) \rightarrow (k_2, j_2)} = P[(I_{k_2}, j_2) | (I_{k_1}, j_1)]$ . To compute these probabilities, we start with the fate of a cell just after firing, computing  $p_{(3, j) \rightarrow (k, 1)}$  for each relevant  $(j, k)$ . First, note that since all cells fire from a state of the form  $(I_3, j)$  for some  $j \leq 3$  and all firing cells are reset together to  $w_{RK}^E$  regardless of where they fired from,  $p_{(3, j) \rightarrow (k, 1)}$  is independent of  $j$ . In this example, with  $g_{inh} = 0.12$ , we have  $p_{(3, j) \rightarrow (1, 1)} = P[T_1 \in [20, 50)]$ , where  $T_1$  denotes the time from reset to the onset of the next excitatory input. Further,  $P[T_1 \in [20, 50)] = 3/4$ , since  $T_1$  is selected from a uniform distribution on  $[20, 60]$ . Similarly,  $p_{(3, j) \rightarrow (2, 1)} = 1/4$  and  $p_{(3, j) \rightarrow (k, 1)} = 0$  for all  $k > 2$ .

Next, we seek values for  $p_{(1, 1) \rightarrow (k, 2)}$  for each  $k \geq 2$  and  $p_{(2, 1) \rightarrow (k, 2)}$  for each  $k \geq 3$ . We have

$$p_{(1, 1) \rightarrow (2, 2)} = P[T_1 + T_2 + 10 \in [50, 75.5) | T_1 \in [20, 50)],$$

where  $T_2 + 10$  denotes the second IEL, with the input duration of 10 msec written out explicitly. This can be computed as the ratio of two areas, either geometrically or by integration, leading to the result that  $p_{(1, 1) \rightarrow (2, 2)} = 2601/9600$ . Since  $N = 3$  for  $s_{inh} = 0$ , it follows that  $p_{(1, 1) \rightarrow (3, 2)} = 6999/9600$ ,

and that  $p_{(2,1) \rightarrow (3,2)} = p_{(2,2) \rightarrow (3,3)} = 1$ . This completes the calculation for  $s_{inh} = 0$ . The corresponding transition matrix for  $s_{inh} = 0$  is thus

$$P^0 = \begin{bmatrix} 0 & 0 & 2601/9600 & 6999/9600 & 0 \\ 0 & 0 & 0 & 1 & 0 \\ 0 & 0 & 0 & 0 & 1 \\ 3/4 & 1/4 & 0 & 0 & 0 \\ 3/4 & 1/4 & 0 & 0 & 0 \end{bmatrix}, \tag{A.1}$$

where the states of the Markov chain are the states (1, 1), (2, 1), (2, 2), (3, 2), (3, 3).

Similar calculations yield the transition matrix

$$P_n^0 = \begin{bmatrix} 0 & 0 & .1474 & .8526 & 0 \\ 0 & 0 & 0 & 1 & 0 \\ 0 & 0 & 0 & 0 & 1 \\ .8576 & .1424 & 0 & 0 & 0 \\ .8576 & .1424 & 0 & 0 & 0 \end{bmatrix} \tag{A.2}$$

for states (1,1), (2,1), (2,2), (3,2), (3,3) in the case of normally distributed IEIs, also discussed in section 6.

**Remark 11.** The time intervals associated with each  $I_k$  are independent of the number of inputs received since the last spike, and hence uniquely defined, under the assumption of input-independent evolution of  $w$  (see remark 8). Without this assumption, to each bin, we could associate different time intervals based on the number of inputs received since the last spike. Once this is done, the calculations proceed as discussed here, with appropriate adjustment of the limits of integration in equation 3.5.

**Appendix B: TC Cell with  $s_{inh} = 1$**  \_\_\_\_\_

The case  $s_{inh} = 1$  requires more analytical computations than the case  $s_{inh} = 0$ , since  $N = 5$  for  $s_{inh} = 1$ . In this case,  $p_{(5,j) \rightarrow (k,1)}$  are identical to  $p_{(3,j) \rightarrow (k,1)}$ , computed for  $s_{inh} = 0$  above, and are nonzero only for  $k = 1, 2$ . The states for  $s_{inh} = 1$  correspond to times [20,50), [50,80), [80,110), [110,128), [128,  $\infty$ ) (see remark 11). Similar to the previous case, with the input duration of 10 msec again included explicitly,

$$p_{(1,1) \rightarrow (2,2)} = P[T_1 + T_2 + 10 \in [50, 80) | T_1 \in [20, 50)] = 3/8,$$

with  $p_{(1,1) \rightarrow (3,2)} = 1/2$  and  $p_{(1,1) \rightarrow (4,2)} = 1/8$  by analogous calculations. Along the same lines,

$$p_{(2,1) \rightarrow (3,2)} = P[T_1 + T_2 + 10 \in [80, 110) | T_1 \in [50, 60)] = 5/8,$$

while  $p_{(2,1) \rightarrow (4,2)} = 37/100$  and  $p_{(2,1) \rightarrow (5,2)} = 1/200$ . As we proceed further, certain probability calculations become more involved, because membership in a state may be achieved by more than one path. For example, we see already that a cell may reach state  $(I_3, 2)$  from  $(I_1, 1)$  or from  $(I_2, 1)$ . Thus, continuing to use  $T_i$  to denote the times between the offset of one input and the onset of the next, we have

$$\begin{aligned} p_{(3,2) \rightarrow (4,3)} &= P[T_1 + T_2 + T_3 + 20 \in [110, 128) | T_1 \in [20, 50) \text{ and } T_1 + T_2 \\ &\quad + 10 \in [80, 110)] + P[T_1 + T_2 + T_3 \\ &\quad + 20 \in [110, 128) | T_1 \in [50, 60) \text{ and } T_1 + T_2 + 10 \in [80, 110)] \\ &= 2123/14,250. \end{aligned}$$

The full set of calculations reveals that the transition matrix  $P^I$  for  $s_{inh} = 1$  has the form

$$P^I = \begin{bmatrix} 0 & 0 & \frac{3}{8} & \frac{1}{2} & 0 & \frac{1}{8} & 0 & \cdot & \cdot & \cdot & 0 \\ 0 & 0 & 0 & \frac{5}{8} & 0 & \frac{37}{100} & 0 & 0 & \frac{1}{200} & 0 & 0 & 0 \\ 0 & 0 & 0 & 0 & \frac{1}{4} & 0 & \frac{6011}{13500} & 0 & 0 & \frac{2057}{6750} & 0 & 0 \\ 0 & \cdot & \cdot & \cdot & 0 & \frac{2123}{14250} & 0 & 0 & \frac{12127}{14250} & 0 & 0 \\ 0 & \cdot & \cdot & \cdot & 0 & \frac{243}{10000} & 0 & 0 & \frac{9757}{10000} & 0 \\ 0 & \cdot & \cdot & \cdot & 0 & 0 & 0 & 1 & 0 & 0 \\ 0 & \cdot & \cdot & \cdot & 0 & 0 & 0 & 0 & 1 & 0 \\ 0 & \cdot & \cdot & \cdot & 0 & 0 & 0 & 0 & 0 & 1 \\ \frac{3}{4} & \frac{1}{4} & 0 & \cdot & 0 \\ \frac{3}{4} & \frac{1}{4} & 0 & \cdot & 0 \\ \frac{3}{4} & \frac{1}{4} & 0 & \cdot & 0 \\ \frac{3}{4} & \frac{1}{4} & 0 & \cdot & 0 \end{bmatrix} \quad (\text{B.1})$$

where the states of the Markov chain are  $(1,1)$ ,  $(2,1)$ ,  $(2,2)$ ,  $(3,2)$ ,  $(3,3)$ ,  $(4,2)$ ,  $(4,3)$ ,  $(4,4)$ ,  $(5,2)$ ,  $(5,3)$ ,  $(5,4)$ , and  $(5,5)$ .

Similar calculations yield the transition matrix

$$P_n^I = \begin{bmatrix} 0 & 0 & .2548 & .7249 & 0 & .0203 & 0 & 0 & 0 & 0 \\ 0 & 0 & 0 & .7352 & 0 & .2642 & .0006 & 0 & 0 & 0 \\ 0 & 0 & 0 & 0 & .1074 & 0 & 0 & .5612 & .3314 & 0 \\ 0 & 0 & 0 & 0 & 0 & 0 & 0 & .1448 & .8552 & 0 \\ 0 & 0 & 0 & 0 & 0 & 0 & 0 & 0 & 0 & 1 \\ 0 & 0 & 0 & 0 & 0 & 0 & 0 & 0 & 0 & 1 \\ 0 & 0 & 0 & 0 & 0 & 0 & 0 & 0 & 0 & 1 \\ .8576 & .1424 & 0 & 0 & 0 & 0 & 0 & 0 & 0 & 0 \\ .8576 & .1424 & 0 & 0 & 0 & 0 & 0 & 0 & 0 & 0 \\ .8576 & .1424 & 0 & 0 & 0 & 0 & 0 & 0 & 0 & 0 \end{bmatrix} \tag{B.2}$$

for states (1, 1), (2, 1), (2, 2), (3, 2), (3, 3), (4, 2), (4, 3), (5, 2), (5, 3), (5, 4) in the case of normally distributed IEIs, also discussed in section 6.

**Appendix C: Coefficients for Matrix 7.1 in the Case of Time-Dependent Inhibition and Excitation**

---

To calculate the coefficients  $c_{m,n} = p(m)p(n)$  analytically, we compute  $p(1)$ , which is the probability that exactly one excitatory input arrives during an epoch of constant inhibition, and then we compute  $p(m)$  for each  $m = 2, \dots, 6$  as the probability of at most  $m$  inputs arriving minus the probability of at most  $m - 1$  inputs arriving. We stop at  $m = 6$ , since at most six excitatory inputs can arrive during 175 msec, given the IEIs and excitation duration that we consider. Let  $t = 0$  denote the time of inhibitory offset and let  $T_1 \in [125, 175]$  denote the duration of the ensuing time interval on which inhibition remains off. Define  $T_{-1}$  as the time from the last excitatory onset before  $t = 0$  to the first excitatory onset after  $t = 0$ . Let  $T_1$  denote the time of this first excitatory onset. Given that each excitation endures for 10 msec,  $T_{-1} \in [30, 70]$ , while  $T_1 \in [0, T_{-1}]$  (see Figure 7). Finally, let  $T_2$  denote the IEI following the end of the excitatory input that occurs at time  $T_1$ . Since  $T_1 < T_1$  must hold, the value of  $p(1)$  is the probability that  $T_1 + T_2 + 10 > T_1$ . Thus,

$$p(1) = \frac{\int_{125}^{175} \int_{30}^{70} \int_0^{T_{-1}} \int_{\min(T_1 - T_1 - 10, 60)}^{60} dT_2 dT_1 dT_{-1} dT_1}{\int_{125}^{175} \int_{30}^{70} \int_0^{T_{-1}} \int_{20}^{60} dT_2 dT_1 dT_{-1} dT_1} = \frac{27}{51,200}.$$

For  $m > 1$ , each quantity  $p(m)$  is given as the ratio of two multiple integrals as well, with one additional nested integral in each, relative to those used to calculate  $p(m - 1)$ . Since these integrals can be evaluated exactly, we obtain exact fractional representations for each, but to save

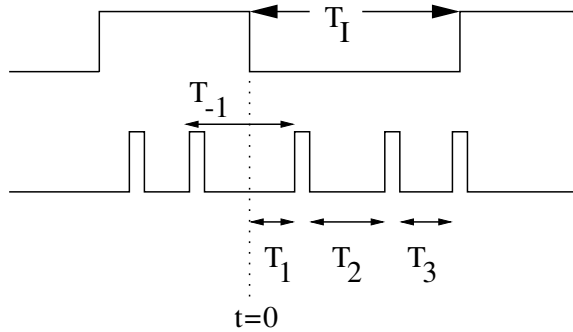


Figure 7: Notation for the calculation of the probabilities  $p(m)$ . Note that the actual number of excitatory inputs arriving during the interval of constant inhibition will be between one and six.

space, we simply give decimal approximations here:  $p(2) \approx .1985$ ,  $p(3) \approx .6075$ ,  $p(4) \approx .1875$ ,  $p(5) \approx .0060$ ,  $p(6) \approx 4.731 \times 10^{-6}$ .

## Acknowledgments

---

We received partial support for this work from National Science Foundation grants DMS-0414023 to J.R., and DMS-0244529, ATM-0417867 and a GEAR grant from the University of Houston to K.J. We thank the anonymous reviewers for comments that helped improve the clarity of the letter.

## References

---

- Aizenman, C. D., Akerman, C. J., Jensen, K. R., & Cline, H. T. (2003). Visually driven regulation of intrinsic neuronal excitability improves stimulus detection in vivo. *Neuron*, *39*(5), 831–842.
- Anderson, M., Postpuna, N., & Ruffo, M. (2003). Effects of high-frequency stimulation in the internal globus pallidus on the activity of thalamic neurons in the awake monkey. *J. Neurophysiol.*, *89*, 1150–1160.
- Babadi, B. (2005). Bursting as an effective relay mode in a minimal thalamic model. *J. Comput. Neurosci.*, *18*, 229–243.
- Brown, P., Oliviero, A., Mazzone, P., Insola, A., Tonali, P., & Lazzaro, V. D. (2001). Dopamine dependency of oscillations between subthalamic nucleus and pallidum in Parkinson's disease. *J. Neurosci.*, *21*, 1033–1038.
- Chance, F., Abbott, L., & Reyes, A. (2002). Gain modulation from background synaptic input. *Neuron*, *35*, 773–782.
- Chow, C., & Coombes, S. (2006). Existence and wandering of bumps in a spiking neural network model. *SIAM J. Dyn. Syst.*, *5*, 552–574.

- Coombes, S., & Osbaldestin, A. (2000). Period-adding bifurcations and chaos in a periodically stimulated excitable neural relaxation oscillator. *Phys. Rev. E*, *62*, 4057–4066.
- Cowan, R. L., & Wilson, C. J. (1994). Spontaneous firing patterns and axonal projections of single corticostriatal neurons in the rat medial agranular cortex. *J. Neurophysiol.*, *71*(1), 17–32.
- De Schutter, E. (1999). Using realistic models to study synaptic integration in cerebellar Purkinje cells. *Rev. Neurosci.*, *10*, 233–245.
- Desai, N. S., Cudmore, R. H., Nelson, S. B., & Turrigiano, G. G. (2002). Critical periods for experience-dependent synaptic scaling in visual cortex. *Nat. Neurosci.*, *5*(8), 783–789.
- Doi, S., Inoue, J., & Kumagai, S. (1998). Spectral analysis of stochastic phase lockings and stochastic bifurcations in the sinusoidally forced van der Pol oscillator with additive noise. *J. Stat. Phys.*, *90*(5/6), 1107–1127.
- Fellous, J. M., Houweling, A. R., Modi, R. H., Rao, R. P., Tiesinga, P. H., & Sejnowski, T. J. (2001). Frequency dependence of spike timing reliability in cortical pyramidal cells and interneurons. *J. Neurophysiol.*, *85*(4), 1782–1787.
- Haken, H. (2002). *Brain dynamics: Synchronization and activity patterns in pulse-coupled neural nets with delays and noise*. Berlin: Springer-Verlag.
- Hashimoto, T., Elder, C., Okun, M., Patrick, S., & Vitek, J. (2003). Stimulation of the subthalamic nucleus changes the firing pattern of pallidal neurons. *J. Neurosci.*, *23*, 1916–1923.
- Hoel, P. G., Port, S. C., & Stone, C. J. (1972). *Introduction to stochastic processes*. Boston: Houghton Mifflin.
- Huertas, M., Groff, J., & Smith, G. (2005). Feedback inhibition and throughput properties of an integrate-and-fire-or-burst network model of retinogeniculate transmission. *J. Comp. Neurosci.*, *19*, 147–180.
- Hunter, J. D., & Milton, J. G. (2003). Amplitude and frequency dependence of spike timing: Implications for dynamic regulation. *J. Neurophysiol.*, *90*(1), 387–394.
- Ichinose, N., Aihara, K., & Judd, K. (1998). Extending the concept of isochrons from oscillatory to excitable systems for modeling excitable neurons. *Int. J. Bif. Chaos*, *8*(12), 2375–2385.
- Keener, J. P., Hoppensteadt, F. C., & Rinzel, J. (1981). Integrate-and-fire models of nerve membrane response to oscillatory input. *SIAM J. Appl. Math.*, *41*(3), 503–517.
- Kuramoto, Y. (1984). *Chemical oscillations, waves, and turbulence*. Berlin, Springer-Verlag.
- Lasota, A., & Mackey, M. C. (1994). *Chaos, fractals, and noise: Stochastic aspects of dynamics* (2nd ed.). New York: Springer-Verlag.
- LoFaro, T., & Kopell, N. (1999). Timing regulation in a network reduced from voltage-gated equations to a one-dimensional map. *J. Math. Biol.*, *38*(6), 479–533.
- Magnin, M., Morel, A., & Jeanmonod, D. (2000). Single-unit analysis of the pallidum, thalamus, and subthalamic nucleus in parkinsonian patients. *Neuroscience*, *96*, 549–564.
- Nini, A., Feingold, A., Slovlin, H., & Bergman, H. (1995). Neurons in the globus pallidus do not show correlated activity in the normal monkey, but phase-locked

- oscillations appear in the MPTP model of parkinsonism. *J. Neurophysiol.*, *74*, 1800–1805.
- Othmer, H., & Watanabe, M. (1994). Resonance in excitable systems under step-function forcing. I. Harmonic solutions. *Adv. Math. Sci. Appl.*, *4*, 399–441.
- Othmer, H., & Xie, M. (1999). Subharmonic resonance and chaos in forced excitable systems. *J. Math. Biol.*, *39*, 139–171.
- Person, A. L., & Perkel, D. J. (2005). Unitary IPSPs drive precise thalamic spiking in a circuit required for learning. *Neuron*, *46*(1), 129–140.
- Raz, A., Vaadia, E., & Bergman, H. (2000). Firing patterns and correlations of spontaneous discharge of pallidal neurons in the normal and tremulous 1-methyl-4-phenyl-1,2,3,6-tetrahydropyridine vervet model of parkinsonism. *J. Neurosci.*, *20*, 8559–8571.
- Rubin, J. E., & Terman, D. (2002). Geometric singular perturbation analysis of neuronal dynamics. In B. Fiedler (Ed.), *Handbook of dynamical systems* (Vol. 2, pp. 93–146). Amsterdam: North-Holland.
- Rubin, J. E., & Terman, D. (2004). High frequency stimulation of the subthalamic nucleus eliminates pathological thalamic rhythmicity in a computational model. *J. Comput. Neurosci.*, *16*, 211–235.
- Ruskin, D. N., Bergstrom, D. A., Kaneoke, Y., Patel, B. N., Twery, M. J., & Walters, J. R. (1999). Multisecond oscillations in firing rate in the basal ganglia: Robust modulation by dopamine receptor activation and anesthesia. *J. Neurophysiol.*, *81*(5), 2046–2055.
- Schreiber, S., Fellous, J.-M., Tiesinga, P., & Sejnowski, T. J. (2004). Influence of ionic conductances on spike timing reliability of cortical neurons for suprathreshold rhythmic inputs. *J. Neurophysiol.*, *91*(1), 194–205.
- Smith, G., & Sherman, S. (2002). Detectability of excitatory versus inhibitory drive in an integrate-and-fire-or-burst thalamocortical relay neuron model. *J. Neurosci.*, *22*, 10242–10250.
- Somers, D., & Kopell, N. (1993). Rapid synchronization through fast threshold modulation. *Biol. Cybern.*, *68*, 393–407.
- Somers, D., Todorov, E., Siapas, A., Toth, L., Kim, D., & Sur, M. (1998). A local circuit approach to understanding integration of long-range inputs in primary visual cortex. *Cerebral Cortex*, *8*, 204–217.
- Steriade, M., Nunez, A., & Amzica, F. (1993a). A novel slow (< 1 Hz) oscillation of neocortical neurons in vivo: Depolarizing and hyperpolarizing components. *J. Neurosci.*, *13*(8), 3252–3265.
- Steriade, M., Nunez, A., & Amzica, F. (1993b). Intracellular analysis of relations between the slow (< 1 Hz) neocortical oscillation and other sleep rhythms of the electroencephalogram. *J. Neurosci.*, *13*(8), 3266–3283.
- Stone, M. (2004). *Varied stimulation of a relaxation oscillator*. Unpublished master's thesis, University of Houston.
- Stuart, G., & Häusser, M. (2001). Dendritic coincidence detection of EPSPs and action potentials. *Nat. Neurosci.*, *4*, 63–71.
- Tateno, T., & Jimbo, Y. (2000). Stochastic mode-locking for a noisy integrate-and-fire oscillator. *Phys. Lett. A*, *271*, 227–236.
- Taylor, H. M., & Karlin, S. (1998). *An introduction to stochastic modeling* (3rd ed.). San Diego, CA: Academic Press.

- Tiesinga, P. (2005). Stimulus competition by inhibitory interference. *Neural Comput.*, *17*, 2421–2453.
- Tiesinga, P., Jose, J., & Sejnowski, T. (2000). Comparison of current-driven and conductance-driven neocortical model neurons with Hodgkin-Huxley voltage-gated channels. *Phys. Rev. E*, *62*, 8413–8419.
- Tiesinga, P., & Sejnowski, T. (2004). Rapid temporal modulation of synchrony by competition in cortical interneuron networks. *Neural Comput.*, *16*, 251–275.
- Tiesinga, P. H. E., & Troups, J. V. (2005). The possible role of spike patterns in cortical information processing. *J. Comput. Neurosci.*, *18*(3), 275–286.
- van Vreeswijk, C., & Sompolinsky, H. (1998). Chaotic balanced state in a model of cortical circuits. *Neural Comput.*, *10*, 1321–1371.
- Xie, M., Othmer, H., & Watanabe, M. (1996). Resonance in excitable systems under step-function forcing. II. Subharmonic solutions and persistence. *Physica D*, *98*, 75–110.

---

Received November 9, 2005; accepted August 18, 2006.